

Solar Photovoltaic Energy Storage System

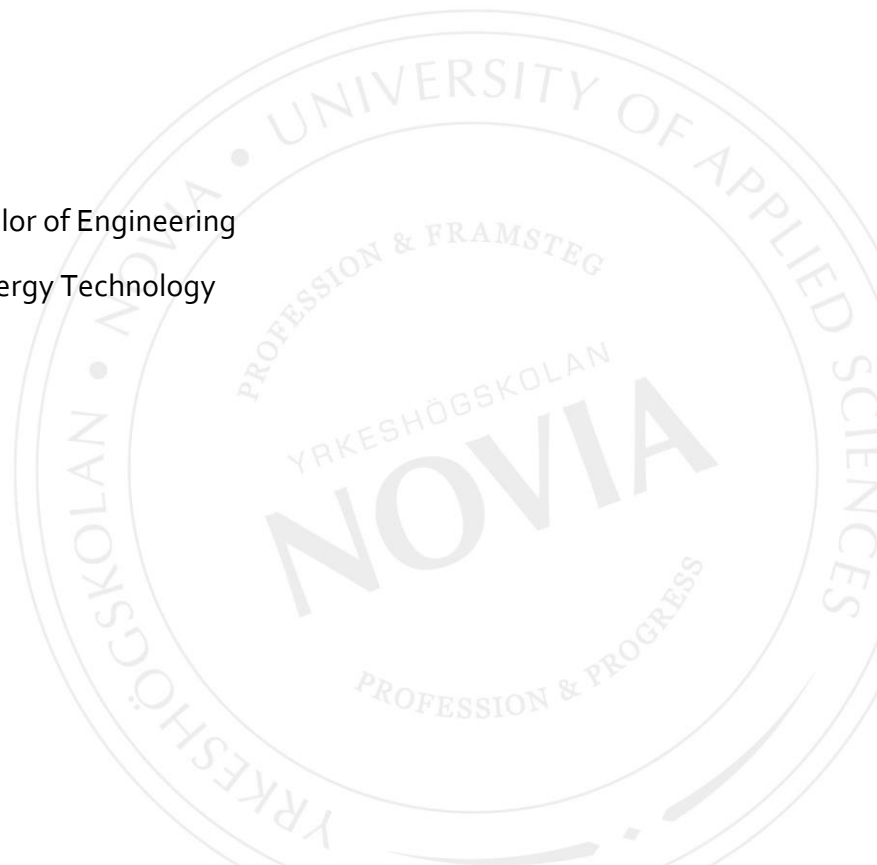
Anna Cànovas Trujillo

Adrià Francés Vigatà

Bachelor Thesis for Bachelor of Engineering

Degree Programme in Energy Technology

Vaasa, 2021



BACHELOR'S THESIS

Authors: Anna Cánovas Trujillo and Adrià Francés Vigatà

Degree Programme: Electronic and Automatic Industrial Engineering

Specialization: Energy Technology

Supervisor(s): Philip Hollins and Hans Lindén

Title: Solar Photovoltaic Energy Storage System

Date 21th May 2020

Number of pages: 67

Appendices: 2

In recent years, the price point for both photovoltaic module and battery storage capacity has decreased dramatically and encouraged uptake by both utility and domestic scale users. Novia University of Applied Sciences commissioned this project to develop a renewable energy system capable of collecting data automatically as an educational tool. For this proposal for developing a LabVIEW program and design an intuitive interface for students to control the system will be required. Moreover, ensuring its proper functioning will be essential.

Literature research was undertaken to obtain background information on all components of the system - especially photovoltaic panels and batteries. Subsequent simulation tasks were carried out to understand how the Modbus TCP communication works to start programming with LabVIEW. Once the software was developed, the focus was on the interface, the information it should contain and how to adapt it for an intuitive design. To validate the proper functioning of the system, final tests were performed on the solar panels and the battery.

Possible component alternatives have been assessed throughout the thesis and concluded that they were not feasible at the scale of this project. In conclusion, all the system proved successful, no anomalies were observed, and it will be able to be incorporated as an educational tool for further projects.

Language: English

Keywords: LabVIEW, PV panels, Batteries, Modbus, QModMaster.

Table of contents

1	Introduction	1
1.1	Aims and Objectives	3
1.2	Document Structure	4
2	Background Information	5
2.1	Principle of solar energy	5
2.1.1	Silicon	6
2.1.2	Doping N and P semiconductors	7
2.1.3	P-N Junction	9
2.2	Types of PV panels	12
2.2.1	Monocrystalline	12
2.2.2	Polycrystalline	13
2.2.3	Thin-film	13
2.3	Batteries	15
2.3.1	Primary cells	15
2.3.1.1	Zinc-carbon cell	15
2.3.1.2	Alkaline cell	17
2.3.2	Secondary cells	19
2.3.2.1	Nickel-cadmium cell	19
2.3.2.2	Lithium-ion cell	21
2.3.2.3	Lead-acid cell	24
2.4	Equipment	27
2.4.1	Color Control GX	27
2.4.2	Battery monitor BMV-700	29
2.4.3	Multi Compact 12/800/35-15 Inverter Charger	30
2.4.4	MPPT regulator 75/10	32
2.4.5	PV Solar Panel NM35WFL	33
2.4.6	AGM Battery 51Ah	35
2.4.7	System assembly	37
2.5	Modbus	39
2.5.1	QModMaster	40
2.5.2	First steps with QModMaster	40
2.6	LabVIEW	42
3	Methodology	44
3.1	Developing LabVIEW Program	44
3.1.1	First steps with LabVIEW	44
3.1.2	Data selection	44

3.1.3	Program development	46
3.2	Designing LabVIEW Interface	50
4	Results: Testing the final system	52
4.1	PV panel analysis	52
4.1.1	Scenario 1: Sunny weather	54
4.1.2	Scenario 2: Cloudy weather	56
4.1.3	Scenario 3: Rainy weather	58
4.1.4	PV panel possible alternatives	60
4.2	Battery analysis	61
4.2.1	Discharge	61
4.2.2	Battery possible alternatives	63
5	Discussion	65
6	Conclusions	67
7	List of references	68
8	Appendices	77
8.1	Appendix I – Overview table of the used components	77
8.2	Appendix II – Block diagram of the LabView program	80

List of figures

Figure 1. Greenhouse gas emissions by sector	1
Figure 2. Cumulative installed PV power	2
Figure 3. Price of a Li-ion battery pack, volume-weighted average	2
Figure 4. General properties of silicon	6
Figure 5. N-type doping	8
Figure 6. P-type doping	8
Figure 7. PV Solar cell structure	9
Figure 8. PN junction	10
Figure 9. PN junction forward biased	11
Figure 10. PN junction reverse biased	12
Figure 11. Zinc-carbon battery scheme	17
Figure 12. Alkaline battery scheme	19
Figure 13. Nickel-cadmium battery	21
Figure 14. Parts of a lithium-ion battery	22
Figure 15. Lead-Acid Battery	25
Figure 16. Color Control GX component	27
Figure 17. BMV-700 monitor	29
Figure 18. Multi Compact 12/800/35-15 Inverter Charger	30
Figure 19. MPPT 75/10 regulator	32
Figure 20. PV Solar Panel NM35WFL	33
Figure 21. Material structure of the NM35WFL solar panel	34
Figure 22. AGM Battery 51Ah	35
Figure 23. Front appearance of the system	37
Figure 24. Rear appearance of the system.....	37
Figure 25. Electrical schematic of the system assembly.....	38
Figure 26. Modbus data transmission	39
Figure 27. AD4ETH: Ethernet A/D converter	40
Figure 28. Power supply connected via Modbus to Qmodmaster	41
Figure 29. LabVIEW tools palette.....	42
Figure 30. Data selection.....	45
Figure 31. Modbus TCP data collection block diagram.....	46
Figure 32. Data collection summary in LabVIEW.....	48
Figure 33. Creation of a spreadsheet with the data block diagram.....	48
Figure 34. Final Interface of the project.....	50
Figure 35. Location of the PV panel.....	53
Figure 36. PV Voltage (V) in sunny weather	54
Figure 37. Meteorological data from 3th May	55
Figure 38. PV Voltage (V) in cloudy weather	56
Figure 39. Meteorological data from 7th May	57
Figure 40. PV Voltage (V) in rainy weather	58
Figure 41. Meteorological data from 10th of May	59
Figure 42. AGM 51Ah battery discharge.....	62
Figure 43. Typical Li-ion discharge voltage curve	63
Figure 44. Discharge voltage in different deep cycle batteries.....	64
Figure 45. Final block diagram in LabVIEW (part 1)	80
Figure 46. Final block diagram in LabVIEW (part 2)	81
Figure 47. Final block diagram in LabVIEW (part 3)	81
Figure 48. Final block diagram in LabVIEW (part 4)	81

List of tables

Table 1. Comparison between different types of solar panels.....	14
Table 2. Zinc-carbon battery summary table.....	17
Table 3. Alkaline battery summary table.....	19
Table 4. Nickel-cadmium battery summary table.....	21
Table 5. Li-ion battery summary table.....	23
Table 6. Lead-acid battery summary table.....	26
Table 7. Technical specifications of the CCGX.....	28
Table 8. Technical specifications of the BMV-700 monitor.....	29
Table 9. Technical specifications of the inverter.....	31
Table 10. Technical specifications of the charger.....	31
Table 11. General technical specifications of the Multi compact 12/800/35-15 Inverter Charger.....	31
Table 12. Technical specifications of the MPPT regulator 75/10.....	33
Table 13. Technical specifications of the NM35WFL.....	34
Table 14. Technical specifications of the AGM 51Ah battery.....	36
Table 15. Selected values that will be taken in every sample of the program.....	45

1 Introduction

The greenhouse gases and related emissions are released into the atmosphere mainly by human activity and contribute to overall global warming. These gases work like a heat-trapping blanket, trapping heat and reflecting it to the Earth. The atmosphere has been altered as a result causing the planet's average temperature to rise. The average global surface temperature has increased approximately 1.18 degrees Celsius over the last century, mostly driven by rising carbon dioxide emissions to the atmosphere and further human activities (Earth Science Communications Team, 2021). The sector that contributes most to the increase of these greenhouse gases is the energy sector (Our World in Data, 2013), for the creation of electricity and heat, with the burning of fossil fuels (coal and oil derivatives) and the processes involved in industrial activities. Today, thousands of devices use electricity as a source of energy, whether in the form of direct current or alternating current, and their use has led to a large increase in the demand for electricity consumption. For this reason, using renewable energy sources has a vital role in reducing the impact of global warming (Process Industry Forum, 2019). All projections are based on European countries' plans to install renewable energy sources, with the latest update showing a variety of strategies to achieve the EU's collective target of 20 per cent of energy from renewable sources by 2020 (European Environment Agency, 2011).

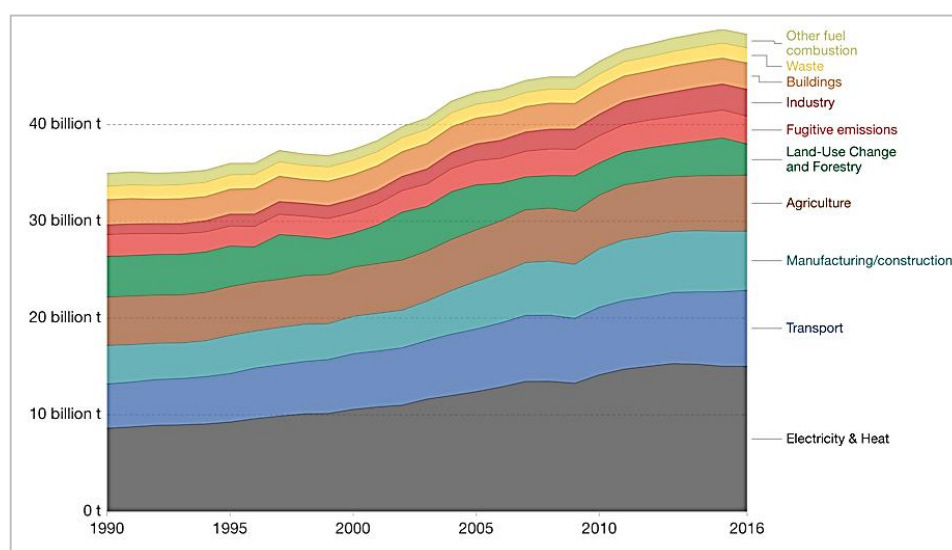


Figure 1. Greenhouse gas emissions by sector (Our World in Data, 2013)

This has led to massive growth in renewables, especially striking in the case of solar PV (both utility and household) due to increased affordability (Figure 2) and legislative support.

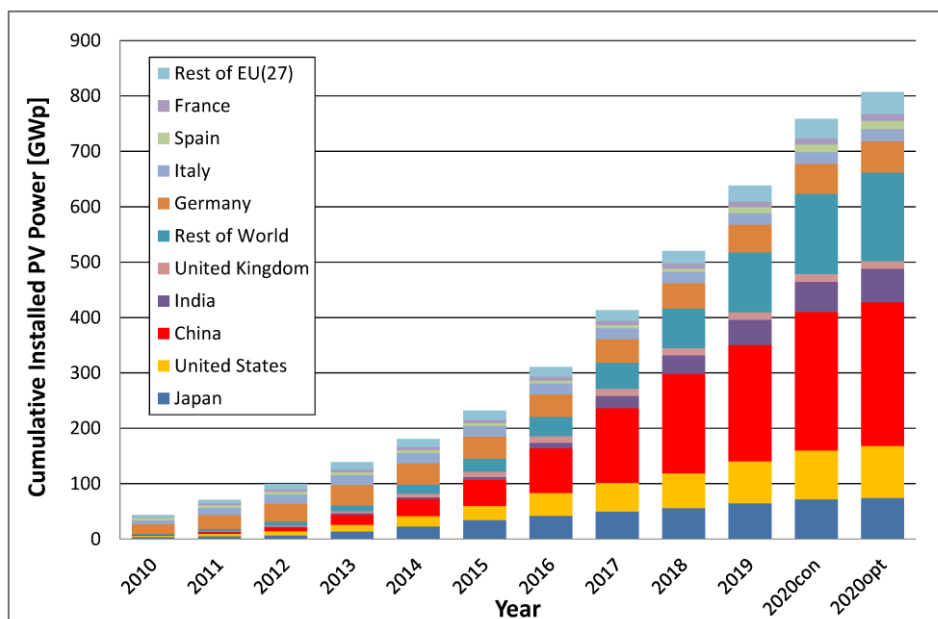


Figure 2. Cumulative installed PV power (GWp) (Jäger-Waldau, 2020)

Figure 2 shows the exponential increase in the installation of solar installations in recent years. However, like wind, solar PV generation is intermittent, its high penetration significantly affects the operation of the electricity system (Shin and Roh, 2020). Therefore, many governments have also started to focus on energy storage systems. Of the range of energy storage systems available, batteries are becoming the most affordable in terms of price. In the last decade, the price has dropped by 88% (Figure 3).

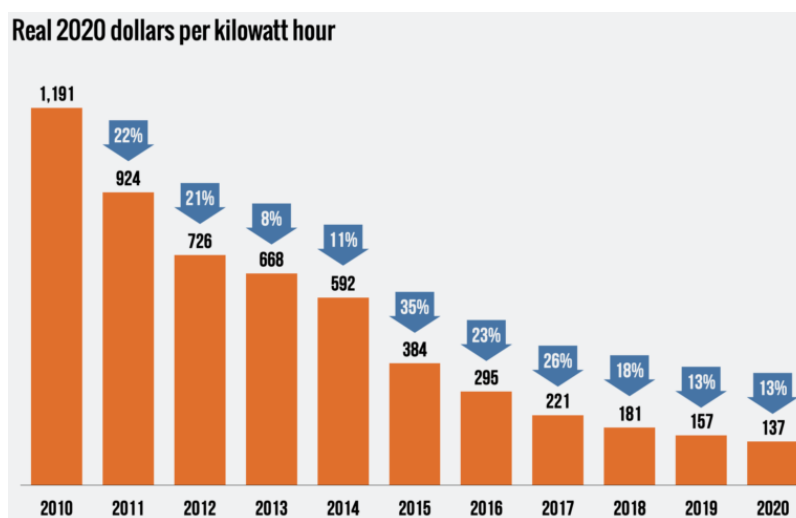


Figure 3. Price of a Li-ion battery pack, volume-weighted average (Lee, 2020)

Figure 3 demonstrates the steady decline in the price of batteries per kWh over time, with the prediction that this is on a pace to reach a value below \$100 (82€) by 2024 (Lee, 2020).

The combination of decreasing price point for both PV module and battery storage capacity is proving increasingly attractive to both utility and domestic scale users. It is estimated that the market for distributed solar PV and battery storage is expected to exceed \$49 billion (approximately 40.36 billion euros) by 2026 and reach 27.4 GW in turnover (Fernández, 2017).

1.1 Aims and Objectives

Novia University of Applied Sciences has been active in developing training tools for use in teaching renewable energy technologies. Such tools are an important part of the learning methods used in the education sector in Finland (CCE Finland OY, 2021).

Previous work has been undertaken with a range of solar PV testing and integration tools, but have not included options for incorporating battery storage. In addition, there was also no programmed software to automatically collect data in excel sheets.

This project was commissioned by Novia University of Applied Sciences. The aim of the project is to develop a renewable energy system capable of collecting data automatically under various conditions for educational purposes. This educational tool features a battery as well as a PV panel and could be applied for data analysing (inputs and outputs) such as voltages, currents, power, etc. The objectives of the project are:

- Develop a LabVIEW program capable of automatically collecting data to Excel.
- Design an intuitive and user-friendly interface for students to control the system.
- Undertake different tests to ensure the proper functioning and efficiency of the system.

1.2 Document Structure

The first section *2. Background Information* provides an overview of the theory concerning PV panels and batteries – the main components of the system. In addition, it describes the other components used and displays them as they are connected. Finally, information about the programs needed for the development of the educational tool's software is provided.

Secondly, in section *3. Methodology* presents how the program has been developed with LabVIEW and how the interface design has been done. Therefore, part of the practical side of the project can be found here.

Finally, in the last section *4. Results: Testing the final system*, the proper functioning of the system is analysed with different tests; the PV solar panels in three different scenarios and the battery facing a discharge. The results obtained are compared with possible alternatives available in the market for the overall improvement of the system in the future.

2 Background Information

In order to have a well-developed practical part of the project – with the performance of several system tests – it is essential to have previous knowledge about the topics covered, in this case, batteries and solar panels. In both cases, various types will be analysed to theoretically corroborate that the system is being implemented with the right components. Then, in section 4. *Results: Testing the final system*, the components will be subjected to different experiments to prove again the researched theory.

In terms of energy generation - with solar panels - we will discuss how energy is converted from the sun's rays, the chemical element most present in solar panels and the structure of solar panels. Finally, the different types of solar panels available on the market will be discussed and analysed for possible future use in the system.

On the other hand, as far as energy storage is concerned - with batteries - the chemical reactions that take place inside batteries will be discussed. Different types of cells will be shown to see how they have improved over time up to the battery that will be used in the system, the AGM battery and its main competitor, the lithium battery.

2.1 Principle of solar energy

Solar energy starts, as the name suggests, with the sun. The solar panels (also known as photovoltaic panels) operate to convert sunlight, which is made up of particles of energy called photons, to electricity that can be utilised to power electrical loads (Dhar, 2017). Unlike solar panels, solar thermal energy is often used to heat water or air in a very simple way: the roof panels are the collectors of the sunlight, which warm the liquid in the pipes and convey it to the cylinder, ready for use (Energy.gov, 2021). Even the principle behind both types of technologies is the same - they absorb raw energy from the sun and use it to create usable energy. Both options are available for energy storage, but for electrical energy storage, photovoltaics offer distinct advantages in terms of cost and efficiencies. For these reasons, it will be solar photovoltaic and electrical storage that will be the focus of this thesis

The majority of solar panel choices currently available suit one of the following three types: monocrystalline, polycrystalline (also referred to as multi-crystalline) and thin-film. The

options vary in terms of manufacturing, appearance, performance, costs and most suitable installations of each type of solar panel. For the production of electricity, solar cells are manufactured from a semiconductor material that transforms light into electricity, silicon is the most common material used as a semiconductor (Energysage.com, 2021). The "semi" part of the word refers to the fact that electricity can be conducted better than an insulator (ceramics, plastic, rubber, wood, etc.) but not as well as a good conductor such as a metal (silver, copper, gold, zinc, nickel, etc.) (Energy.gov, 2020). Nowadays, more than 90% of the existing solar cell market consists of silicon (Greenmatch.co.uk, 2021).

2.1.1 Silicon

Silicon is the second most abundant material on Earth (after oxygen and before aluminium) and the most widely utilised semiconductor in computer chips (Energy.gov, 2020). Silicon is a metalloid chemical element, with atomic number 14 and located in group 14 of the periodic table of elements with the symbol *Si* (see Figure 4). Its atomic mass is 28.0855u that means the mass of a single particle, and its electron configuration is [Ne]3s² 3p² with 4 electrons in the outer orbital (Figure 4) (Connor, 2020). Two allotropes of silicon exist at room temperature: amorphous and crystalline (PubChem, 2021).

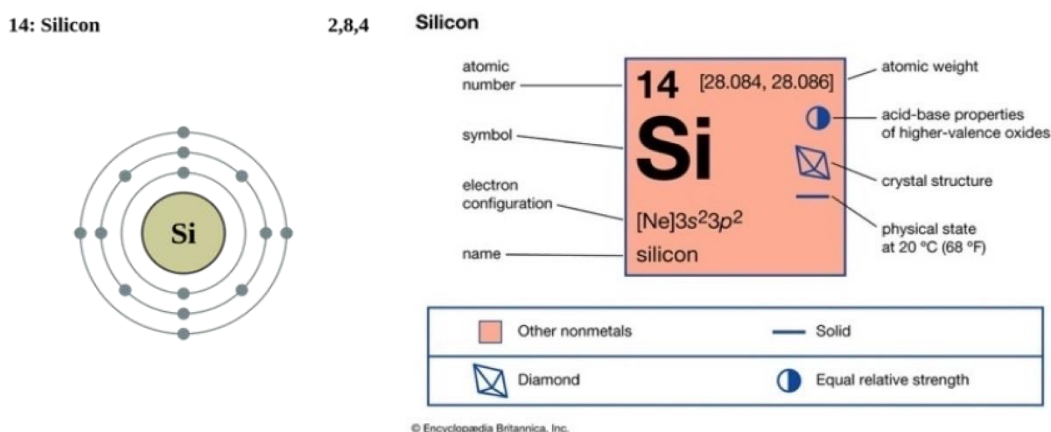


Figure 4. General properties of silicon (Britannica, 2021)

The silicon crystalline cells are composed of silicon atoms joined together to create a crystalline lattice. The lattice gives an ordered pattern that enables light to be converted into electricity more efficiently (Energy.gov, 2020). However, pure crystalline silicon conducts electricity poorly, because it is essentially a semiconductor material. To overcome this problem, the silicon in a solar cell includes impurities, i.e., different atoms have been purposely blended onto the silicon atoms to enhance its ability to absorb the

sun's energy and turn it into electricity (Greenmatch.co.uk, 2021). The name given to this procedure in where impurities are purposely added to an intrinsic semiconductor is doping. Two types of impurities are present in the doping of silicon: N-type (where electrons have a negative charge) and P-type (where electrons have a positive charge) (Granath, 2020).

2.1.2 Doping N and P semiconductors

As mentioned above, doping is the process of introducing impurities within a semiconductor crystal for the defined modification of the conductivity.

Taking gallium and arsenic mixed separately with silicon, for example, the atom of gallium has one less electron than an atom of silicon in the outer orbital (so, a gallium atom has 3 electrons in its outer orbital), while an arsenic atom has one electron more in the outer orbital (so, an arsenic atom has 5 electrons in its outer orbital). So, two scenarios occur:

- When the arsenic atoms are placed between many silicon atoms, extra electrons will be present in the structure, resulting in the creation of an electron-rich layer (Greenmatch.co.uk, 2021).

This is N-type doping, where arsenic or phosphorus is doped into silicon in low amounts. These two elements have five electrons in their outer orbitals, which means that four of the five orbital electrons are bound to their silicon neighbouring atoms, leaving one 'free electron' which will move when an electrical voltage (electron flow) will be applied (Basic Electronics Tutorials, 2013). So, the "N" (negative) side contains an excess of electrons. In Figure 5 an example of this bonding of electrons to neighbouring atoms, introduced as impurities to silicon, can be seen graphically with an antimony atom which also contains five electrons in its outer orbital.

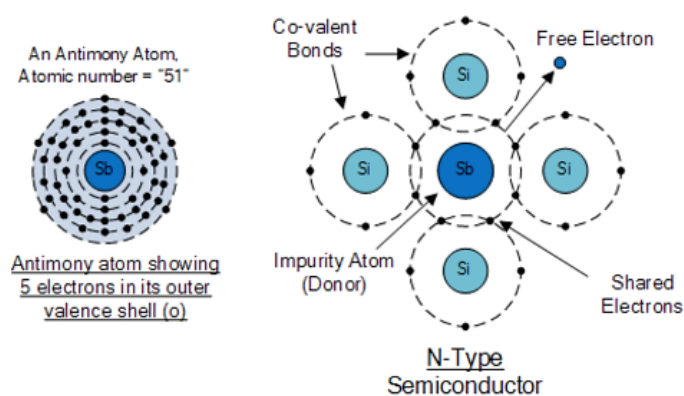


Figure 5. N-type doping (Basic Electronics Tutorials, 2013)

- Instead, when using gallium atoms, a lack of electrons will occur, which means that an electron-poor layer will be created (Greenmatch.co.uk, 2021).

This is P-type doping, in which boron or gallium is added. Each of these elements holds three electrons in its outer orbitals so, when combined in the silicon lattice, holes are formed in the valence band of the silicon atoms because the fourth closed bond cannot be formed. So, the electrons in the valence band move, and the holes move in the opposite direction to the movement of the electrons. In this way, because the dopant is locked in the crystal lattice, it is only the positive charges that can move. These semiconductors are known as P-type because of the positive holes (Basic Electronics Tutorials, 2013). In Figure 6 an example of this bonding of electrons to neighbouring atoms, introduced as impurities to silicon, can be seen graphically with a boron atom which also contains three electrons in its outer orbital.

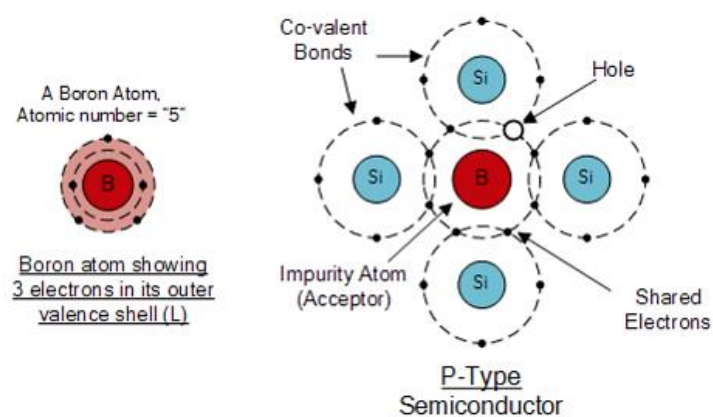


Figure 6. P-type doping (Basic Electronics Tutorials, 2013)

In a solar cell, these two types of layers are placed next to each other, creating an electric field (Figure 7). When sunlight strikes the solar cell, they absorb the photons and in doing so initiate an electric current where the flow and movement of electrons take place. The energy stimulates electrons that leave holes. These migrate to the electrodes of the cell due to the presence of the electric field. In this way, electricity is generated.

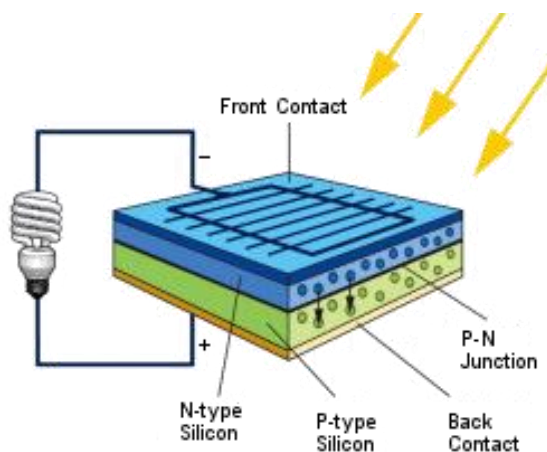


Figure 7. PV Solar cell structure (Glenergy Solar, 2015)

In Figure 7, it is shown graphically how in the N-layer where there can be found the arsenic and silicon (there are "additional" electrons) move to the P-layer of gallium and silicon (where there are "missing" electrons, there are the holes) so, electrons migrate across the junction allowing electric current to pass through in only one direction.

2.1.3 P-N Junction

The PN junction is a border area between the two types of semiconductor materials mentioned above, P-type and N-type, placed into a single semiconductor crystal. With no external voltage applied to a PN junction, an equilibrium condition is reached in which a potential difference is formed across the junction (Ling, Sanny and Moebis, 2016). This potential difference is known as the built-in potential V_{bi} (Analog Devices, 2017).

At the junction, near the bond region, the free electrons of the N-type are drawn to the positive holes of the P-type. Diffusing towards the P-type, they combine with the holes and cancel each other out. The movement of the electrons towards the P-type side exposes positive ion nuclei on the N-type side, while the movement of the holes towards the N-type side exposes negative ion nuclei (anions) on the P-type side, resulting in an electron field

at the junction and the formation of the depletion region or layer (Figure 8) (Electronics Tutorials, 2013). With the progression of the diffusion process, the space charge zone increases in width, leading to deeper layers in the crystals on both sides of the junction (Proyecto investigación de Tecnología, 2021).

This means that in the PN junction band there is; on the one hand, negative charge (in the P-zone), where gallium and silicon are combined, and on the other hand positive charge (in the N-zone), where arsenic and silicon are combined. The accumulation of positive ions in the N-zone and negative ions in the P-zone (Figure 8), creates an electric field E that will actuate against the free electrons in the N-zone with a certain displacement force, which will resist the current of electrons and eventually stop them (Honsberg and Bowden, 2021). Both zones before this movement of electrons were neutrally charged. This junction can be called a diode, as it is known in electronics.

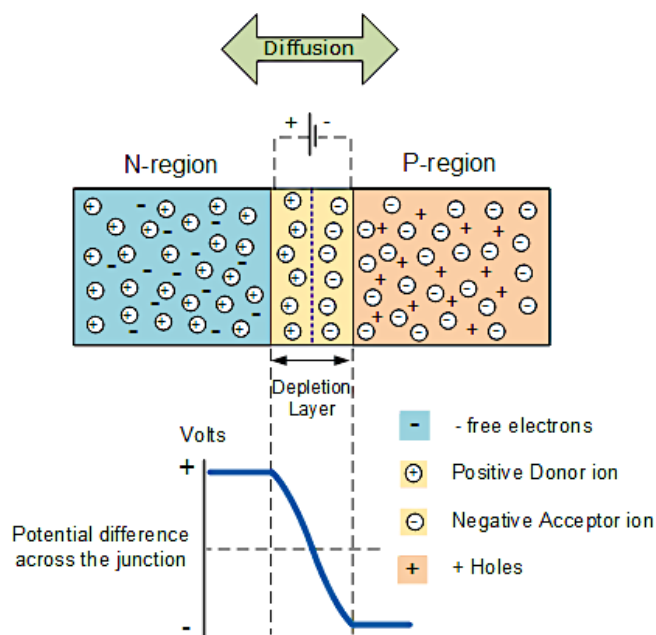


Figure 8. PN junction (Basic Electronics Tutorials, 2013)

Therefore, when a new electron from the N-zone tries to cross into the P-zone, it will be confronted with the negative charge of the depletion layer in P which will stop it from passing, as equal charges repel each other. It could be said that this region acts as a barrier. The electron-hole recombination ends at this point and no more electrical conduction takes place.

Finally, to get more electrons to pass through the depletion layer and conduction to occur, it is necessary to supply them with the energy needed to overcome the repulsive force of the negative ions in the P-zone (Gsu.edu, 2021). This energy can be supplied by a power source such as a battery or a power supply connected to the junction or diode as can be seen in Figure 9. There are two bias conditions with the given power supply when a diode is connected in a circuit: the forward bias condition and the reverse bias condition (Marino, 2020). If a diode is connected in a circuit, with its anode at the positive terminal and its cathode at the negative terminal of the power supply, it is known as biased condition (Figure 9) but when connected in reverse - the diode is connected with its anode at the negative terminal and its cathode at the positive terminal of the power supply - the connection is known as reverse biased (Figure 9).

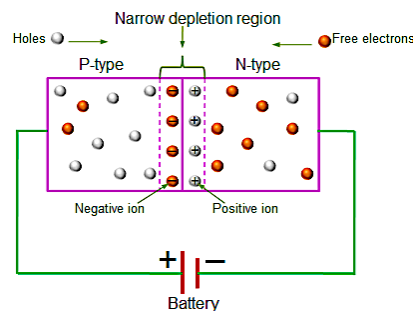


Figure 9. PN junction forward biased (Shaik, 2013)

The battery in forward biased condition lowers the potential barrier of the space charge region, allowing the electron current to flow across the junction (Figure 9), i.e. the directly polarised diode conducts electricity, contributes to higher conduction. The external voltage necessary for reaching above the existing potential barrier is highly dependent upon the specific type of semiconductor material employed and the actual temperature of the semiconductor. At room temperature, the voltage through the depletion layer for silicon is normally around 0.6 - 0.7 V and around 0.3 - 0.35 V for germanium. (Basic Electronics Tutorials, 2013).

In Figure 9 it can be observed a direct polarization (forward bias) of the PN junction with the battery by giving up free electrons to the N-zone and attracting valence electrons from the P-zone, a constant electric current flow through the diode until the battery is consumed.

If a voltage with indirect polarity is applied (reverse bias), it would further prevent the flow of electrons across the junction as it would pull the electrons away from the junction, stopping conduction (Figure 10). A diode cannot conduct in reverse bias (Marino, 2020).

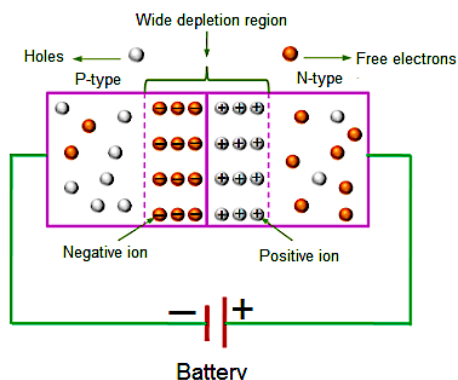


Figure 10. PN junction reverse biased (Shaik, 2013)

2.2 Types of PV panels

There is a wide variety of solar panels on the market today, but depending on the installation being studied, one type or another will be more suitable (Sendy, 2017). Each solar panel has its characteristics and there are many factors to consider before choosing which type to use.

Most solar panels currently on the market for solar energy systems can be classified into three categories depending on the method used to manufacture them. These categories are monocrystalline solar panels, polycrystalline solar panels and thin-film solar panels.

2.2.1 Monocrystalline

The wafers of monocrystalline solar panels are made from cylinders of single-crystal silicon. They are manufactured with the Czochralski method, this gives them their high efficiency but a lot of silicon is scrapped because to fit more wafers in the panel, the silicon cylinders are cut on four sides, the removed parts are discarded, and therefore have the characteristic shape of the cells (Energysage, 2021). This way the space on the panel is used efficiently. Since the cell is made up of a single crystal, the electrons generating a flow of current have more space to circulate. The result of this is the high efficiency of this type of solar panel.

Being made of single-cell silicon, monocrystalline solar panels have a darker appearance, this will allow them to capture a little bit more solar energy (Sandhu, 2019).

2.2.2 Polycrystalline

The main difference between monocrystalline and polycrystalline panels is in their manufacture, while monocrystalline panels were made of a single cell, polycrystalline panels are made of fused silicon remnants, the fact that it is not pure silicon gives it a slightly bluish colour (Marsh, 2017). And instead of having it in cylinders, it can be shaped as desired from the beginning, so it is put in squares to occupy as much space as possible. This process is much faster than manufacturing monocrystalline cells, and also cheaper as single-cell silicon is not used.

Heat, so warm weathers, affect their efficiency a bit more than monocrystalline ones. However, this is a minor issue, and users do not normally need to take it into account as the difference is minimal in most scenarios (Andres, 2017).

2.2.3 Thin-film

Thin-film solar cells (TFSC) are manufactured by depositing one or more thin layers of photovoltaic material on a substrate.

They can be classified according to the composition of the layers applied to them (EnergySage, 2020). The most commonly used are amorphous silicon, cadmium telluride and copper indium gallium selenide.

- Amorphous Silicon is the cheapest and most widely used option even though they have a rather low efficiency of around 7%.
- Cadmium telluride is a cheap alternative as well and with higher efficiency of about 11%, but the raw material used is quite uncommon and they are rarely manufactured.
- Copper indium gallium selenide is the most expensive type as they have reached efficiencies higher than 20%.

They are easy and cheap to build, as less material is needed for its production, so mass production is simple. They are lightweight and can be flexible so they are less likely to break but their lifetime is shorter as they tend to degrade more rapidly than the crystalline types. This kind of solar panel has much lower efficiency and therefore would take up much more space to produce the same power output as either of the other two varieties.

To summarize the specific characteristics of each type of photovoltaic solar panel depending on its manufacture, the following table has been constructed containing information on the advantages and disadvantages of each type compared to the others.

Table 1. Comparison between different types of solar panels.

Solar Panel Type	Monocrystalline	Polycrystalline	Thin-film
Advantages	High efficiency (15-20%) Sleeker aesthetics Take up less space.	Low cost Fast manufacture	Very cheap Most Aesthetic
Disadvantages	High cost High silicon waste	Low efficiency (13-17%)	Very low efficiency (7-13%) Fast degrade
Characteristics	Obtained from pure silicon (Czochralski)	Fewer crystallisation phases and blueish surface	Lightweight and flexible

In the system to be designed, the efficiency of the solar panel is important but not decisive, other characteristics such as price and low weight (see Table 1) are more relevant as it will be easier to transport it and it can be moved to carry out different analyses. For this reason, the panel to be included in the equipment for the project, with which samples will be taken and used in the analysis, will be of the thin-film type.

2.3 Batteries

The fundamental principle of a battery consists of the oxidation-reduction (redox) reactions of certain chemicals, one of them losing electrons (oxidising) and the other gaining electrons (reducing). So, reactions involving electron transfers (Lumen, 2011). Oxidation-reduction processes are simultaneous, meaning that for one chemical species to lose electrons, another species must be present to accept them (Chemistry LibreTexts, 2013). The batteries contain chemical cells that present a positive pole (cathode) and a negative pole (anode), along with electrolytes that allow and facilitate the electrical flow. The anode and cathode never contact each other; they are connected through the electrolyte (Sciencing, 2020). These cells convert chemical energy into electrical energy through a reversible or irreversible process, depending on the type of battery. In this way, two types of cells are classified: primary and secondary cells.

2.3.1 Primary cells

Non-rechargeable batteries or primary cells are those which, once the reaction has taken place, cannot return to their original state, thus exhausting their capacity to store electric current (OpenStax, 2016). So, once used, these batteries have to be thrown away because the electrochemical processes that made the battery produce energy cannot be reversed.

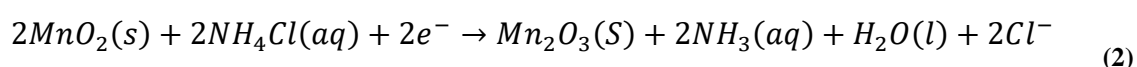
2.3.1.1 Zinc-carbon cell

A common primary battery is the zinc-carbon dry cell. It provides approximately 1.5 volts of direct current from an electrochemical reaction between zinc and manganese dioxide. A carbon rod collects the current from the manganese dioxide electrode, giving the cell its name (Google Books, 2011). The zinc can serve as a container as well as a negative electrode (Figure 11). A carbon rod is the positive electrode and is enclosed by manganese (IV) oxide paste, zinc chloride, ammonium chloride, carbon powder and a small quantity of water (Chemistry LibreTexts, 2015). The anode reaction is represented as the standard oxidation of zinc:



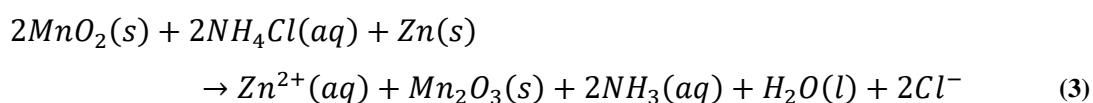
The electrons move from the zinc section to the manganese (IV) oxide section, resulting in a deficit of electrons in the zinc section and an electron excess in the manganese (IV) oxide section. To ensure that the battery functions properly over an extended time, both sections must be in balance.

In the second section, more than one reaction takes place at the cathode - so it is a bit more complex (Chemistry LibreTexts, 2015). Manganese is mixed with carbon powder to increase the electrical conductivity (Science Direct, 2017). In this reaction, manganese is reduced, gaining electrons, and turns its oxidation state from +4 to +3. The sequence of reactions that occur can be represented as follows:



Ammonium chloride is primarily used as a source of H⁺ protons that can balance the excess of electrons in the manganese (IV) oxide section. At the same time, the generated chloride ions Cl⁻ (see equation II) balance the lack of electrons in the zinc section. In addition, on the zinc side, the reaction creates Zn²⁺ (see equation I), which forms insoluble compounds under these conditions. If these compounds accumulate, the electric current will eventually stop. Thanks, once again, to the ammonium chloride, the ammonia NH₃ obtained during the reaction (see equation II) will form a compound with Zn²⁺ which is easily soluble in water.

Finally, the overall reaction of the zinc-carbon battery can be represented as follows:



The overall potential of the cell, as mentioned above, is initially 1.5 V, but gradually drops as the battery is being used. Since the zinc container oxidises, it will eventually lose its contents, which is why this type of battery may not be left with any electrical appliance for prolonged periods (Chemistry LibreTexts, 2015). This type of battery also has a short lifetime and deteriorates significantly in cold weather (Gsu.edu, 2021).

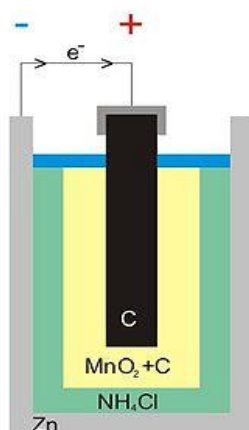


Figure 11. Zinc-carbon battery scheme (Wikiwand, 2021)

A final summary table has been prepared with the chemical compounds and their respective formulas found in each part of the battery.

Table 2. Zinc-carbon battery summary table.

Part of the battery	Compound	Formula
Anode	Zinc	Zn
Cathode	Manganese dioxide	MnO ₂
Electrolyte	Ammonium chloride or zinc chloride dissolved in water	NH ₄ Cl or ZnCl ₂

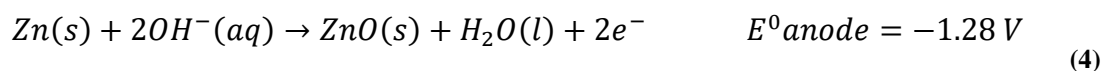
2.3.1.2 Alkaline cell

In the 1950s, alkaline batteries were introduced in part to overcome some of the performance problems of zinc-carbon dry cells (Chemistry LibreTexts, 2015). Alkaline cells and batteries use alkaline electrolytes, as the name suggests, usually potassium hydroxide KOH, instead of the chloride (ammonium chloride or zinc chloride) of zinc-carbon batteries.

As in the zinc-carbon battery, carbon is used in the cathode because manganese dioxide is not a good conductor by itself. It is usually in the form of graphite or acetylene black (Fsu.edu, 2021). The electrolyte, KOH, allows high ionic conductivity. Zinc oxide is often added to stop corrosion of the zinc anode (Nordic Galvanizers, 2019).

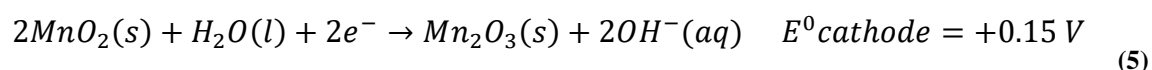
In the simplified form the reactions are:

- At the anode:

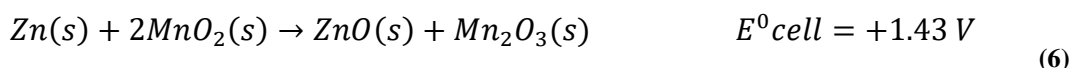


The oxidation of the Zn takes place, losing two electrons.

- At the cathode



The reduction of manganese (IV) oxide occurs, gaining electrons, to give manganese (III) oxide. The overall reaction is:



The alkaline battery has several advantages over the zinc-carbon battery: it can provide three to five times the energy of a dry zinc-carbon battery of similar size (Chemistry LibreTexts, 2015), has a greater energy density, improved performance in continuous and intermittent duty cycles, and lower internal resistance, allowing it to function at higher discharge ratings over a broader temperature operating range (PowerStream, 2021). In addition, it has a longer service life and better performance in cold weather and drainage (Gsu.edu, 2021). On the other hand, the price of these batteries is higher than that of zinc-carbon batteries. Since alkaline batteries are susceptible to leakage of potassium hydroxide, they must also be taken out of devices for long-term storage. Although certain alkaline batteries are rechargeable, the majority are not. Several attempts have been done to recharge an alkaline battery that is not rechargeable and resulted in the battery rupturing and the potassium hydroxide electrolyte escaping (Chemistry LibreTexts, 2015).

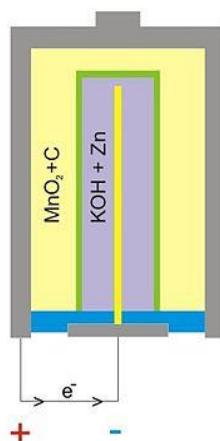


Figure 12. Alkaline battery scheme (Wikiwand, 2021)

A final summary table has been prepared with the chemical compounds and their respective formulas found in each part of the battery.

Table 3. Alkaline battery summary table.

Part of the battery	Compound	Formula
Anode	Zinc powder	Zn
Cathode	Manganese dioxide powder	MnO ₂
Electrolyte	Potassium hydroxide	KOH

2.3.2 Secondary cells

Rechargeable batteries or secondary batteries are those that can receive an electrical energy supply to restore their original chemical composition, so they can be used many times before they are completely depleted. As an example, this occurs when you plug your mobile phone battery into a charger that is connected to a power supply (Palermo, 2015). The most common types of secondary batteries are nickel (nickel-iron, nickel-cadmium and nickel-hydride), lead-acid, lithium-ion (Li-ION) and lithium-polymer (LiPo) batteries.

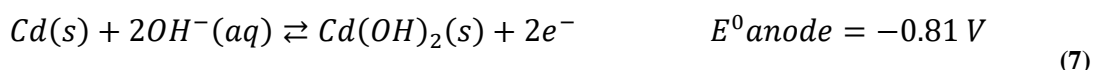
2.3.2.1 Nickel-cadmium cell

Nickel-cadmium (NiCd) batteries (see Figure 13), are made up of a nickel-plated cathode, a cadmium-plated anode and an electrode of potassium hydroxide (Chemistry LibreTexts, 2015). Although the electrolyte, KOH, is only acting as a conductor of ions and is not contributing meaningfully to the cell reaction, occasionally NaOH is employed as an

electrolyte, which does not conduct as well, but does not leach as much through the seal (PowerStream, 2021). To prevent short-circuiting, the positive and negative plates are wound together and inserted into the case. This is a "jelly-roll" design (see Figure 13) which enables the NiCd battery to supply much more current over a similar-sized alkaline battery (Chemistry LibreTexts, 2015).

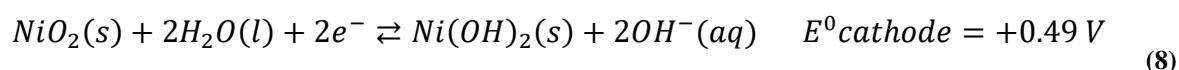
The following reactions take place in this type of battery:

- At the anode



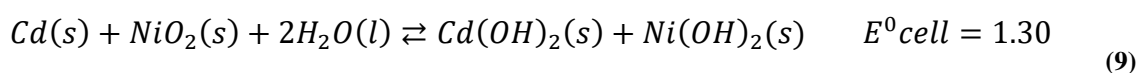
Cadmium metal changes to cadmium hydroxide losing two electrons so, oxidation takes place.

- At the cathode



In this reduction reaction, nickel goes from an oxidation state of +3 to +2.

The general reaction is:



As can be seen from equation 9, the voltage of this battery ranges from 1.2 to 1.5V. If properly treated, a NiCd battery can be recharged around 1000 times (Chemistry LibreTexts, 2015). It also has other advantages like feature good performance in high-discharge and low-temperature applications (PowerStream, 2021). It is one of the most popular batteries for industrial applications as it has many characteristics better than the lead-acid batteries mentioned below. Compared to a lead-acid battery, a NiCd battery is much easier to maintain and has a much longer life, which means less maintenance (K-TRONIX, 2018). The drawbacks are that they are more expensive than lead-acid batteries and offer lower energy densities. One of the best-known limitations is possibly the memory effect, meaning that the cell conserves the previous cycle's characteristics (PowerStream, 2021). Also, cadmium is a toxic heavy metal, so NiCd batteries should not be opened or thrown away and require special care during battery disposal (Osha.gov, 2021).

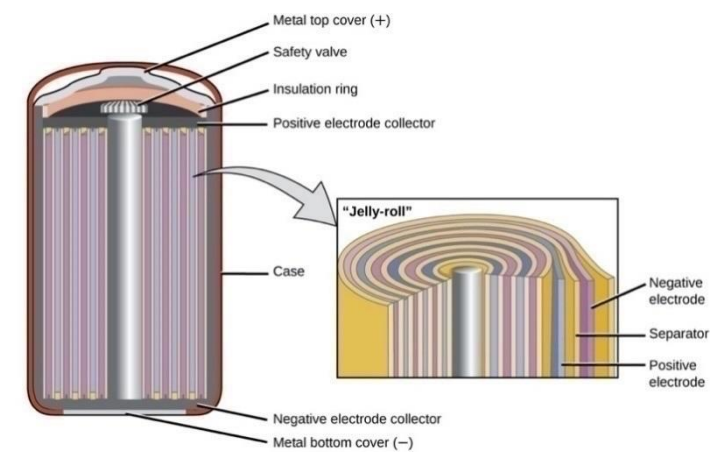


Figure 13. Nickel-cadmium battery (Lumen Learning, 2021)

A final summary table has been prepared with the chemical compounds and their respective formulas found in each part of the battery.

Table 4. Nickel-cadmium battery summary table

Part of the battery	Compound	Formula
Anode	Cadmium	Cd
Cathode	Nickel	Ni
Electrolyte	Potassium hydroxide	KOH

2.3.2.2 Lithium-ion cell

Lithium-ion batteries (LIBs) (Figure 14) represent one of the most popular rechargeable types of batteries widely used in many portable electronic devices such as mobile phones, laptops and digital cameras. Their usage is also employed in electric vehicles and is becoming increasingly popular for military and aerospace uses (Science Direct, 2012). Lithium-ion batteries employ a lithium compound intercalated as the cathode material and usually graphite as the anode material (Figure 14). Cells in experimental studies have also employed lithiated metal oxide such as LiCoO_2 , $\text{NiNi}_{0.3}\text{Co}_{0.7}\text{O}_2$, LiNiO_2 , LiV_2O_5 , $\text{LiV}_6\text{O}_{13}$, LiMn_4O_9 , LiMn_2O_4 , $\text{LiNiO}_{0.2}\text{CoO}_2$ (PowerStream, 2021). Lithium-ion batteries are given the name of their active materials; the words are spelt out in full or abbreviated with their chemical symbols (Battery University, 2019).

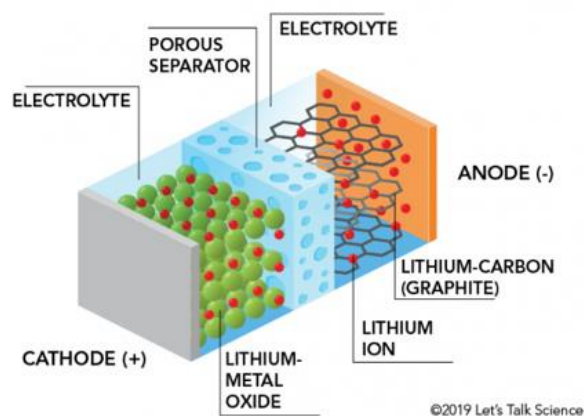


Figure 14. Parts of a lithium-ion battery (Let's Talk Science, 2019)

Nowadays, batteries in common usage contain microporous polyethylene membranes. These are required to separate the electrons from the ions (Science Direct, 2012). Generally, LiPF_6 is used as electrolytes, but it has a corrosion problem with aluminium, and therefore several alternatives are being investigated. One of these is LiBF_4 (PowerStream, 2021).

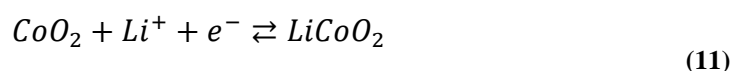
The battery chemistry, performance, cost and safety properties differ for each type of lithium-ion battery. Portable electronic devices mainly employ lithium polymer batteries (with a polymer gel as electrolyte), a lithium cobalt oxide material (LiCoO_2) and a graphite anode, offering together with a high energy density (Mauger and Julien, 2017). The reactions of the lithium cobalt oxide battery (LiCoO_2) will be explained at the different parts of the battery.

The following half-reaction takes place at the anode:



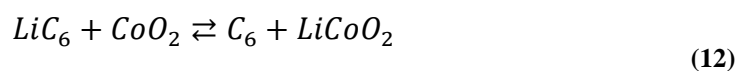
The graphite interlayer compound LiC_6 results in graphite (C_6) and lithium ions, oxidation takes place.

The following half-reaction takes place at the cathode:



In this reduction reaction, cobalt oxide is combined with lithium ions to form lithium cobalt oxide (LiCoO_2).

The general reaction is:



The battery voltage is about 3,7 V (Chemistry LibreTexts, 2015). This type of battery has an enormous energy density, in addition to its lightweight, small size and good performance, but they start failing after two or three years (Battery University, 2011). After they should be replaced and both the production and disposal of lithium-ion batteries have a large impact environmentally, meaning that the longer these batteries last, the better (Let's Talk Science, 2019). Another advantage is their low memory effect (Leonid Leiva, 2013).

One drawback of these batteries is their high capital cost and that lithium is extremely reactive, so manufacturers have to take special safety measures to ensure that the batteries are safe to operate. People may have heard of electronic devices, such as laptops or mobile phones, that burst in flames due to their batteries. To ensure safety, lithium-ion batteries contain a separator that keeps the electrodes of the battery cells away from contacting each other. However, the electrodes can contact each other if this separator is broken or damaged. This can result in a big build-up of heat and, in case of a spark, ignition of the highly flammable electrolyte can occur (Brain, 2021). Manufacturers are constantly improving lithium-ion, new and improved chemical combinations appear approximately every six months (Battery University, 2011). A final summary table has been prepared with the chemical compounds and their respective formulas found in each part of the battery.

Table 5. Li-ion battery summary table

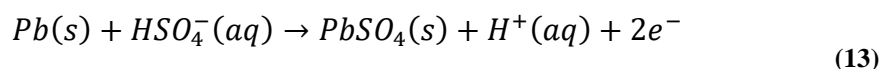
Part of the battery	Compound	Formula
Anode	Carbon compound, graphite	C
Cathode	Lithium oxide	Li ₂ O
Electrolyte	Polymer gel/lithium salt in an organic solvent	

2.3.2.3 Lead-acid cell

The lead-acid battery (Figure 15) was the first type of rechargeable battery to be developed for commercial use. It is cheap and able to produce the high current required by automotive starter motors (Chemistry LibreTexts, 2015). Only a few batteries supply bulk power as cost-effectively as lead-acid, making this battery economical for automobiles, golf cars, forklifts, boats and uninterruptible power supplies (UPS) (Battery University, 2018).

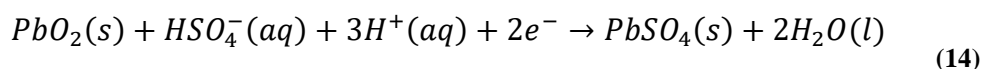
This type of battery is composed of a lead plate coated with lead (II) oxide, PbO_2 , in the positive electrode and a sponge or porous lead in the negative electrode. This lead is porous to facilitate its formation and dissolution (Honsberg and Bowden, 2021). As an electrolyte it has acid sulphuric dissolved in water, the two electrodes are submerged in the solution. The reactions for a lead-acid battery are:

- At the anode



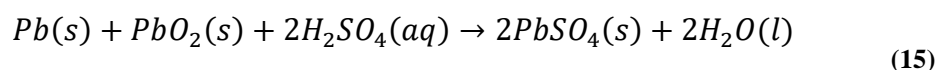
On the negative plate, the sulphate ions in the electrolyte react with the lead, oxidizing it and forming lead sulphate ($PbSO_4$). This reaction releases two electrons.

- At the cathode:



On the positive plate, the sulphate ions react with the lead dioxide, reducing it and forming also lead sulphate. While the hydrogen in the sulphuric acid reacts with the oxygen from the lead dioxide to produce water. The positive plate needs electrons, and of course, obtains them from the negative plate.

The general reaction is:



Such reactions eliminate the sulphuric acid from the electrolyte and eventually stop when there is no more acid or lead (dioxide) remaining to react. Lead sulphate, the by-product of these reactions, coats the plates, damaging them, reducing their capacity and increasing resistance if allowed to form hard crystals (Off Grid Europe, 2017). If large crystals develop

a reduction in the active material of the battery will occur which is responsible for the battery's performance (Battery University, 2016). This is the case where it is colloquially said that the battery is sulphated and has to be replaced with a new one.

Every cell produces 2 V, which means connecting six cells in series will produce a 12 V car battery. Such batteries are typically heavy and contain a caustic liquid electrolyte, however, they are frequently still chosen for their high current density. As these batteries do contain a considerable amount of lead, proper disposal must always be carried out (Chemistry LibreTexts, 2015). They are less long-lasting than nickel and lithium batteries when subjected to deep cycling. As mentioned above, a complete discharge results in stress and each discharge/charge cycle will permanently drain the battery of a slight quantity of capacity. Although this loss is small as long as the battery is in good operating condition, the fading will grow once the performance drops to half of the rated capacity. All batteries are subject to this fading characteristic to different degrees (Battery University, 2018). Li-ion batteries, especially LiFeSO₄ batteries, are technically more advantageous for use in the intermittent solar photovoltaic system than a conventional lead-acid battery.

When lead-acid batteries are being used, small sulphate crystals are produced, but these are normal and not harmful. Nevertheless, upon extended charge deprivation, the amorphous lead sulphate turns into a stable crystalline and is settled on the negative plates. As a result, large crystals develop and reduce the active material in the battery, which is responsible for the battery's performance (Battery University, 2016). This is the case where it is colloquially said that the battery is sulphated and has to be replaced with a new one.

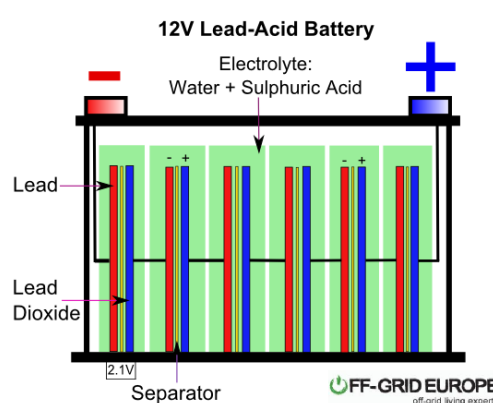


Figure 15. Lead-Acid Battery (Off Grid Europe, 2017)

A final summary table has been prepared with the chemical compounds and their respective formulas found in each part of the battery.

Table 6. Lead-acid battery summary table

Part of the battery	Compound	Formula
Anode	Spongy lead	Pb
Cathode	Lead dioxide	PbO ₂
Electrolyte	Sulphuric acid dissolved in water	H ₂ SO ₄

With the same operating principle as lead-acid batteries, other types of batteries have emerged, such as AGM and Gel batteries (Rebacas, 2020). AGM batteries are sealed batteries whose electrolyte is absorbed in glass fibre separators (Absorbed Glass Material). There is liquid sulphuric acid inside but it is soaked into the glass fibre of the separator, and Gel batteries are also sealed batteries whose electrolyte is a silica gel which is not liquid and the separator material is the same as in AGM, glass fibre.

These batteries, being sealed, have several advantages over traditional lead-acid batteries, including the following: faster charging, longer charge retention in storage, very low sulphation, better withstand partial states of charge, better performance at low temperatures, higher current delivery capability. This makes them a very interesting piece of equipment to be included in the project.

2.4 Equipment

In this section, a description of the different devices used in the project will be found to see the different parts of the equipment and to have a better understanding of how they work. Each part of the system is studied separately and is accompanied by a picture, a description of how it works and a summary of the most important characteristic information extracted from the datasheet of the component. A summary table of all components can be found in Appendix I.

2.4.1 Color Control GX

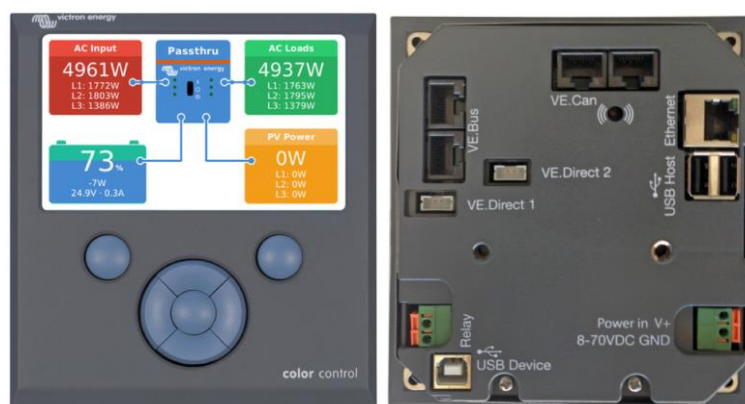


Figure 16. Color Control GX component (Victron Energy, 2020)

The Color Control GX (CCGX) is the centre of communication of the system as it provides real-time information in a quick overview and allows control of the components connected to it, such as the battery and the photovoltaic panel. The system can be controlled from anywhere at any time by connecting to the Color Control GX via the free Victron Remote Management Portal (VRM).

Simply, this component gives you an immediate status overview of your system: battery charge status, power consumption, power harvesting from PV and power supply from the grid/generator.

As mentioned above, the Victron Remote Management System (VRM) offers complete access to the wide-ranging controls and configuration of all system devices that are connected to the CCGX in a remote form, over the internet. Additionally, diagnostic checks

can be performed seamlessly and archived information can be analysed using this application.

It is possible to program the Color Control GX to automatically start a generator, activated by low voltage, high demand, battery charge status or other parameters. In addition, it can be adapted to delay start-up until the end of quiet times, thus avoiding accidental disturbance late at night.

Energy storage systems are managed by the Color Control GX. It maintains the reserve batteries at 100%; activates during power outages; and redirects excess (solar) energy to self-consumption, thus saving money.

In addition, there is a remote console function to control the CCGX from your smartphone and also allows you to communicate with connected equipment from other manufacturers. The CCGX can be updated from the Internet automatically when a new software version is available. It also has multi-language options: English, Czech, German, Spanish, French, Italian, Dutch, Russian, Swedish, Turkish, Chinese and Arabic. The CCGX can be used as a Modbus-TCP gateway for all connected Victron products.

The price of the Color Control GX ranges from 510,00 € and its datasheet can be found in the table in Appendix I.

Table 7. Technical specifications of the CCGX (Victron Energy,2020)

Power supply voltage range	8-70 DC
Current draw	12V DC
Display off	140mA
Outer dimensions	130x120x28mm
Operating temperature range	-20 to 50°C

2.4.2 Battery monitor BMV-700



Figure 17. BMV-700 monitor (Victron Energy, 2020)

The monitor is an accessory to the battery used to know everything about it, battery voltage, current, power, ampere-hours consumed and state of charge are some of the most important characteristics this monitor can read from the battery and show us in real-time. With complex software algorithms, it can also make precise calculations of how much remaining battery is there, and when it will be fully charged.

It is easy to use, but in case you get troubles operating with it, you can use its app “Bluetooth Smart dongle needed”, and control it, program its settings and view the info from the smartphone.

The price of the BMV-700 monitor is about 155,00 € and its datasheet can be found in the table in Appendix I.

Table 8. Technical specifications of the BMV-700 monitor (Victron Energy,2020)

Supply voltage range	6,5-95V DC
Current draw off	<4mA
Battery capacity Ah	1-9.999Ah
Operating temperature range	-40 to 50°C
Dimensions	69x69x31mm

2.4.3 Multi Compact 12/800/35-15 Inverter Charger



Figure 18. Multi Compact 12/800/35-15 Inverter Charger

Typically, in a PV system, the inverter/charger performs two main functions: 1) converting DC power from the batteries into domestic AC power capable of powering standard household appliances and other energy loads, and 2) converting AC power into DC power capable of charging the deep-cycle batteries. Such bi-directional energy exchange is essential for storing and efficiently using the energy collected from photovoltaic systems (Sensata Technologies, 2021).

Victron Energy's 12/800/35 MultiPlus is a true sine wave inverter, a battery charger that has adaptive charging technology and a high-speed AC transfer switch in a single compact unit. Not only does this design save space, but it also makes installation simple by requiring only one set of wires to connect to the battery.

The unit is powerful enough to power most main-powered appliances and features high peak power capability, stable voltage and frequency, and a high-quality sine wave output.

The charger is multi-stage and fully automatic, and the adaptive microprocessor-driven battery management system can be set to several battery types such as wet, AGM, GEL and Li-ion. In this case, it will be used with an AGM battery. It automatically varies the charging

process according to the way the batteries are discharged, making sure that the batteries are always in optimum condition. Two outputs are available for charging; one full power output and a second current and voltage limited output for slow charging a starter battery.

The built-in AC transfer switch provides the function of an uninterruptible power supply (UPS). In case of grid failure, or disconnection of shore or generator power, it automatically activates the inverter and ensures the AC supply to the connected loads. This happens in less than 20 milliseconds and guarantees that the connected sensitive equipment continues to operate without interruption. This function can be deactivated if it is not needed.

The price of the Victron Multi Compact 12/800/35-15 Inverter ranges from 555,44 € and its datasheet can be found in the table in Appendix I.

Table 9. Technical specifications of the inverter (Volt Planet, 2021)

Input voltage range	9,5-17V DC
Output voltage	230V AC
Peak power	1.600W
Max efficiency	92%

Table 10. Technical specifications of the charger (Volt Planet, 2021)

Input voltage range	187-265V AC
Charge voltage (absorption)	14,4V DC
Charge current	35A

Table 11. General technical specifications of the Multi compact 12/800/35-15 Inverter Charger (Volt Planet, 2021)

Operation temperature range	-40 to 65°C
Dimensions	360x240x100mm
Weight	6,4kg

2.4.4 MPPT regulator 75/10



Figure 19. MPPT 75/10 regulator (Victron Energy, 2020)

The main use of the solar regulator is to gather the energy from the PV panels and drive it to the battery, this can be done without a regulator, but the aim of it is to enlarge the life, and to optimize the charge-discharge of the battery.

The regulator works with an adaptive three-step charging, the three steps are bulk, absorption and float. The bulk phase is determined to charge the batteries as fast as possible using the maximum current possible. When the absorption voltage is achieved, it jumps to the next phase which is defined by the constant voltage charge. When only shallow discharges occur, the absorption time is shortened to avoid overcharging the battery. When there's a deep discharge, the absorption time is automatically increased to ensure that the battery is fully recharged. This will extend the battery's life. In addition, the absorption period also ends when the charging current decreases to less than 1A.

The last step is the float charge phase, in this one afloat voltage is given to the battery to maintain it fully charged, if the battery level is dropped during at least 1 minute from the float voltage, it will start a new charging cycle.

The regulator's presence is more noticeable when it is cloudy, because, without it, the charging would be full of peaks and troughs (this would destroy the battery's integrity in few charges), but with it, the charging voltage will be soft and constant.

The price of the MPPT-regulator 75/10 is about 110,00 € and its datasheet can be found in the table in Appendix I.

Table 12. Technical specifications of the MPPT regulator 75/10 (Victron Energy, 2020)

Maximum battery current	10A
Max PV current	13A
Peak efficiency	98%
Charge voltage (absorption)	14,4V
Charge algorithm	Multi-stage adaptive
Continuous load current	15A
Operating temperature range	-30 to 60°C
Dimensions	100x113x40mm

2.4.5 PV Solar Panel NM35WFL

**Figure 20. PV Solar Panel NM35WFL (Tuontitukku.fi, 2021)**

As mentioned above, the solar panel that will be used in the project is of the thin-film type and will be the NM35WFL. The structure of the panel (Figure 21), can be seen is made up of many layers, but the one in charge of collecting the photons coming from the sunlight is made of silicon cells.

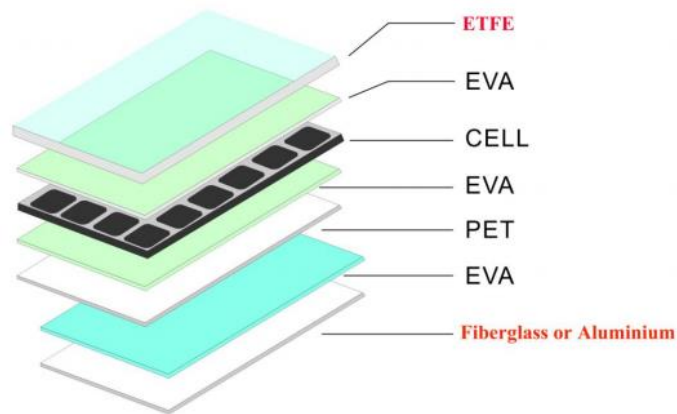


Figure 21. Material structure of the NM35WFL solar panel (Akkupojat.fi, 2021)

This solar panel will allow us to collect data that will help us to analyse the amount of sunlight at our location and more data concerning the viability of solar energy at our workplace. Furthermore, the characteristics of this solar panel (table 13) mean that it is not very expensive and has enough power for the data that will collect the system. For other projects, in bigger installations, this panel would not be adequate as it has pretty low power.

The price of the NM35WFL solar panel ranges from 99 € (Tuontitukku.fi, 2021). and its datasheet can be found in the table in Appendix I.

Table 13. Technical specifications of the NM35WFL (OEM, 2021)

Peak power	35W
Maximum Power Voltage	18V
Maximum Power Current	1.95A
Cell efficiency	17.5%
Number of cells	36
Operating temperature	-20-50°C
Flexible angle	Up to 20°
Weight	1.58kg
Dimensions	700x350x2.5mm

2.4.6 AGM Battery 51Ah



Figure 22. AGM Battery 51Ah (Lillevilla, 2021)

The AGM (Absorbed Glass Material) battery can handle many times more charge and discharge compared to a standard battery. It features good safety because the battery liquid is absorbed in the glass wool between the lead plates, this makes the battery completely leak-proof and maintenance-free. If necessary, it could even be installed indoors, but it is nevertheless recommended installing the AGM batteries outdoors. Ideally somewhere out of the sun, e.g., under the roof, would be the best location. Battery temperature affects the performance of its operation and high temperatures reduce the lifetime of the battery significantly (Aurinkopaneelikauppa, 2021).

The main advantages of AGMs are up to five times faster charging than the flooded (open lead-acid) version and the capacity for deep cycling. The AGM provides an 80 per cent depth of discharge while the flooded version is rated at 50 per cent depth of discharge to achieve the same cycle time (Battery University, 2020).

The price of an AGM battery 51Ah rates from 118€ (Aurinkopaneelikauppa, 2021), and its datasheet can be found in the table in Appendix I.

Table 14. Technical specifications of the AGM 51Ah battery (Aurinkopaneelikauppa, 2021)

System voltage	12V DC
Storage capacity	50 Ah
Self-discharge	Max. 3%
Charging maximum current	12.5A
Charging voltage	14,4-15 V
Temperature range charging	0-40 °C
Temperature range discharging	-20-40 °C
Weight	16,5 kg
Dimensions	230x138x208

2.4.7 System assembly

Once all the parts of the equipment have been mounted and assembled, the final appearance of the system is as shown in Figures 23 and 24, the inverter charger and the regulator are hidden behind the control unit with the wiring (Figure 24) to occupy less space and to make the system easily portable.

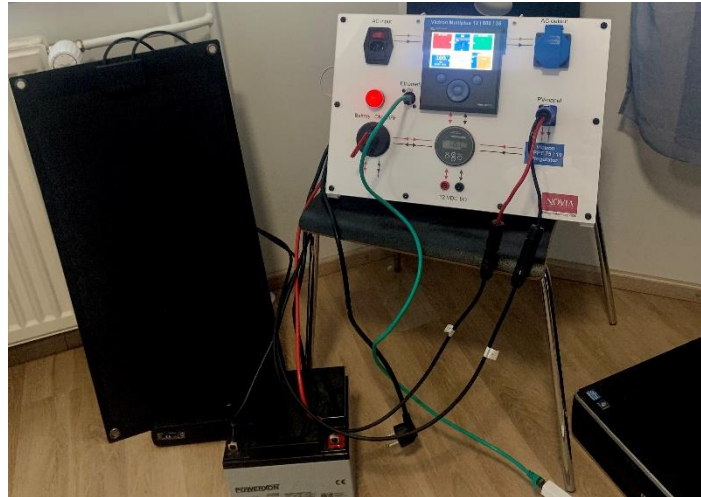


Figure 23. Front appearance of the system

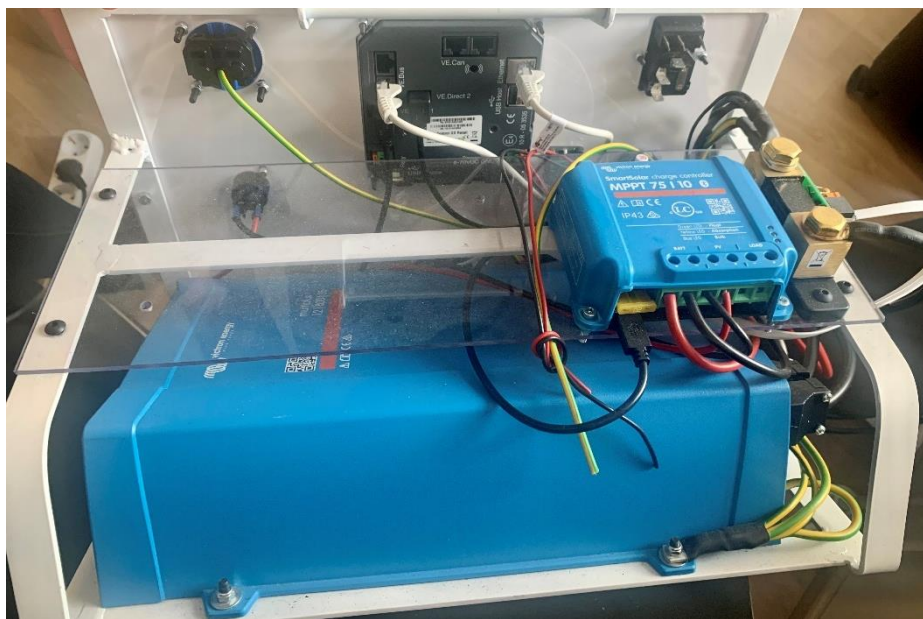


Figure 24. Rear appearance of the system

The overall system connection was schematized using *Circuit Simulator RL V8.4.6*. once all the equipment has been described. This program has been developed by the University of Lleida, edited by the Robotics Laboratory, and is free software: you can redistribute it and

modify it under the terms of the GNU General Public License as published by the Free Software Foundation (Robotica, 2021).

Figure 25 shows the assembly of the system overall with the added changes for electrical safety. It has to be mentioned that this is not a standardised diagram, it is purely an orientation diagram to be able to understand the connections and to find out the circuit's design.

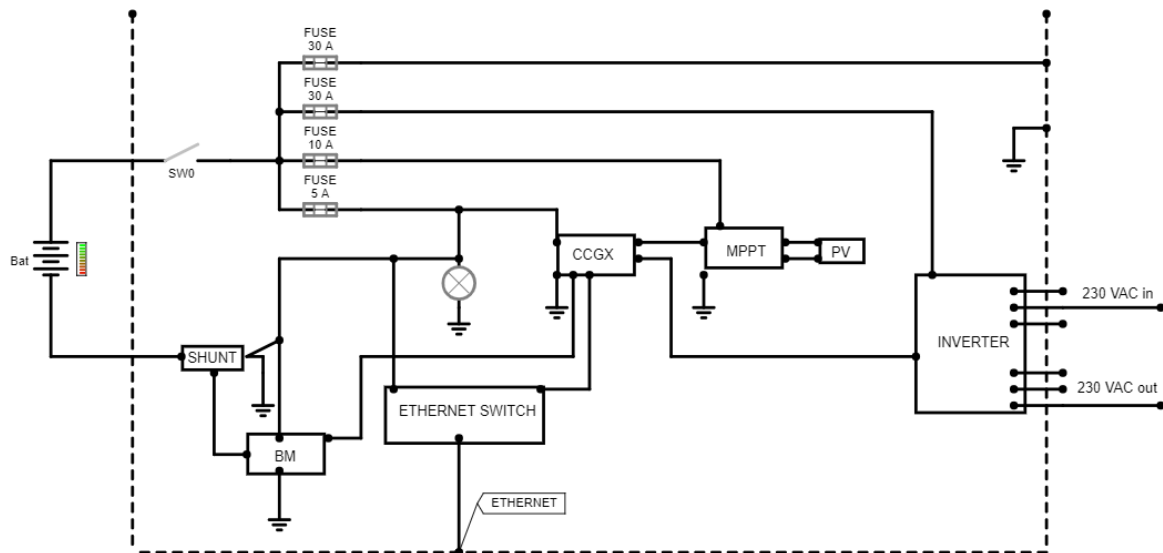


Figure 25. Electrical schematic of the system assembly

As can be seen in Figure 25, four fuses have been added to the circuit to prevent damage to the equipment due to an unexpected overload, or an unforeseen power surge. It can also be appreciated how each of the parts described above is interconnected and how all the equipment will communicate through Ethernet, from where the data for the analysis will be taken.

2.5 Modbus

Modbus is the method used in the project to transmit information between the different electronic devices employed in the system. Modbus is one of the oldest fieldbuses on the market, is an open protocol which means that it is free for manufacturers to incorporate into the equipment without having to pay or to use it for commercial applications. Developed by Modicon (at present Schneider Electric) to manage its programmable logic controllers (PLCs). It is based on a master-slave architecture (Modbus Organisation, 2020).

In Modbus communication, the master transfers commands to the slave devices, which return a reply (Figure 26). Commonly, the master is a human-machine interface (HMI) or a supervisory control and data acquisition (SCADA) system while the slave is a sensor, a programmable logic controller (PLC) or a programmable automation controller (PAC). Different slave devices have different identification addresses. Either the master can send messages and requests to individual slaves or all of them simultaneously. If a response is required, the message is generally sent to a specific slave device. As the slave address is the first byte of the request, it easily lets the slaves know whether to accept or ignore the command (National Instruments, 2021).

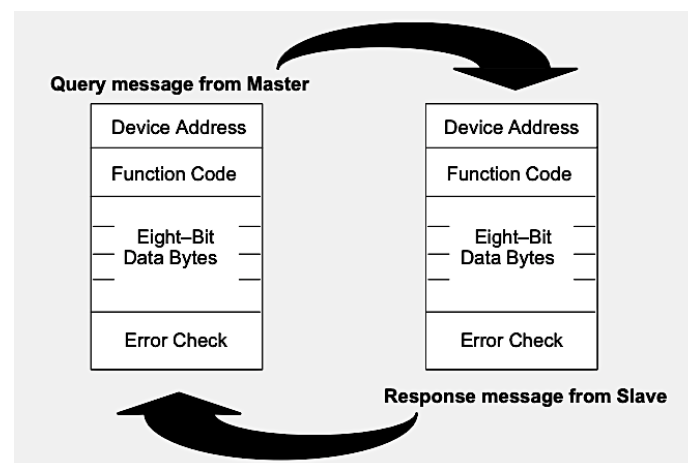


Figure 26. Modbus data transmission (Modicon Modbus Protocol Reference Guide, 1996)

The principal characteristics that have led Modbus to become the most widely used and implemented automation protocol - as well as having been created by one of the largest PLC manufacturers at the time - are its flexibility, message architecture, simple structure, ease of implementation and reliability. An additional reason why Modbus was so

successful was the fact that it could be so easily understood by non-programmers (Tech Step Integration, 2020).

The ability to share Modbus communication over Ethernet is a further important feature of the Serial to Ethernet Connector. It allows remote users to connect to a local Modbus device over an IP-based network.

2.5.1 QModMaster

QModMaster is one of the used programmes throughout the project. It is a free Qt-based application, which simulates a Modbus master device. This tool provides the user with a bus monitor to analyse traffic and a graphical user interface to facilitate communication with ModBus RTU and TCP slaves (Doerffel, 2021). QModMaster allows queries to be made to a specific IP address and port, being able to precisely define each of the fields of the Modbus message. It is a very useful instrument for validations and verifications of the correct operation of a slave device.

2.5.2 First steps with QModMaster

As the final Energy Solar Storage System provides a lot of data of different kinds, units and there was no background knowledge of the programme. Initially, to get in contact with the QModMaster program, an adjustable power supply from the laboratory was used. The power supply was connected to the software via the Ethernet A/D converter (Figure 27) to start transferring the data i.e., the values of voltages and currents measured at the source.



Figure 27. AD4ETH: Ethernet A/D converter (Papouch Store, 2014)

This component allows measuring up to four analogue signals 0-10V or 0(4)-20mA. The values being transferred to the program were known at every moment so, it was easy to see if the software was working well.

In Figure 28 it can be seen how a voltage of 3.5V and a current of 0A (because of the impedance of the converter), were passed to the computer through the converter.

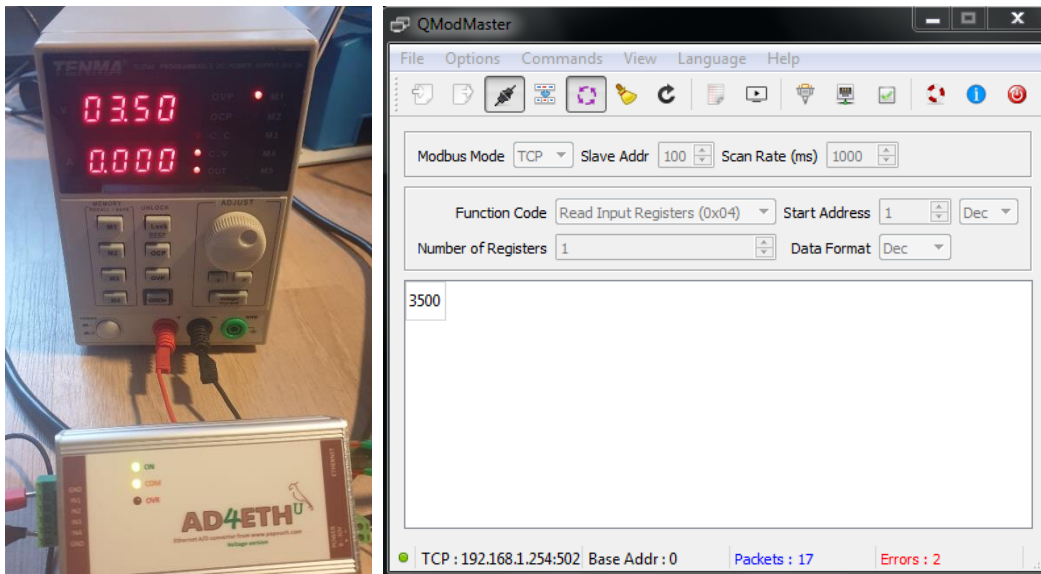


Figure 28. Power supply connected via Modbus to Qmodmaster

As can be seen in Figure 28, the value obtained in QModMaster was 3500 (which is correct in mV), so the units of the data that are obtained must be taken into consideration. It was possible to become familiar with QModMaster and to carry out several tests with it that served for validating the correct operation of the slave device.

2.6 LabVIEW

LabVIEW is a paid software, available via licence <https://www.ni.com/fi-fi/shop/labview.html>, that allows the simulation of more or less complex circuits, including those involving information transfer. It is also called a virtual instrument because its appearance and operation often emulate physical instruments, such as oscilloscopes and multimeters. LabVIEW contains an extensive set of tools for analysis, visualisation, storage and data acquisition. It is also useful for programmers because it contains tools that will help with the debug of the program and simulation of itself.

LabVIEW is primarily used by researchers, engineers, academics and others. Among the companies that are on the list of LabVIEW, customers are John Deere, General Dynamics, Ball Aerospace, Eaton and others. Nowadays it is used mainly by medium-sized companies, followed by small and large organisations and it has a market share of approximately 4.2% (InfoClutch, 2021).

The program is divided into two windows. The left one is the front panel that tries to simulate the real instruments with real inputs, outputs, indicators, instruments, etc. And the right one is the block diagram that contains all the internal information, the programme, configuration and operations involved in the system.

LabVIEW programming is based on a block diagram, which means that it has some blocks defined in the tools palette (Figure 28) and that with the combination of them you can develop the desired programs. The tools palette is quite intuitive and has a lot of different items divided into some categories to make it easier to find them faster. Some of the items

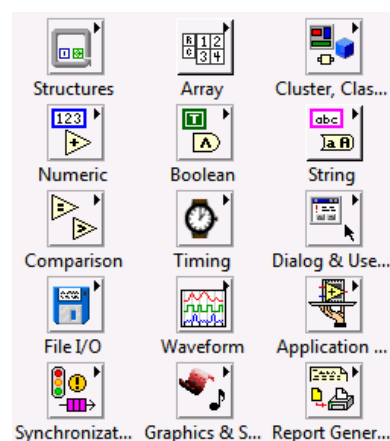


Figure 29. LabVIEW tools palette

are terminals, indicators, controllers, block diagram, Boolean logic items, constants, nodes...

Knowing the items and functions that the program has, can be understood the magnitude and infinity of things that can be done with it, from simple electronic circuits to complex information flow networks.

The cost of the programme currently (11.05.2021) differs depending on the reason for its use, the most basic and student pack which is the one involved in the project costs 420 €/year, but the most complex pack and probably the one used in many companies costs 5690 €/year. A free trial can be downloaded.

3 Methodology

This section covers part of the project, such as the development of the software with LabVIEW and the interface design.

3.1 Developing LabVIEW Program

As there was no previous knowledge of programming with LabVIEW, before developing the program, tests had to be carried out to learn how the program works, and the data that were considered relevant for the project was also selected.

3.1.1 First steps with LabVIEW

Studies, guides and other theses were consulted to get an initial idea of the program. LabVIEW - NOVIA User Guide was the first one, suggested by the lead supervisor, it helped us to know the basic functions of the programme at a very basic level – programming environment, while, loops, graphs, data acquisition, etc. - but including advanced knowledge in a progressive way and explained easily and understandably for the user like filtering and noise removal, storage of the data, etc. The full document can be found in the following MS OneDrive location URL. <https://yhnovia-my.sharepoint.com/>

3.1.2 Data selection

A LabVIEW program has been developed to collect data from the four different units available - system, vebus, solar charger and battery. A preliminary study has been made to select data from an Excel file as it had more than 180 values that could be collected by the system. The most relevant and significant for the study and the user using the interface were carefully chosen for each unit.

dbus-service-name	description	Address	Type	Scalefactor	Range	dbus-obj-path	writable	dbus-unit
com.victronenergy.system	PV - AC-coupled on output L3	810	uint16	1	0 to 65536	/Ac/PvOnOutput/L3/Power	no	W
com.victronenergy.system	PV - AC-coupled on input L1	811	uint16	1	0 to 65536	/Ac/PvOnGrid/L1/Power	no	W
com.victronenergy.system	PV - AC-coupled on input L2	812	uint16	1	0 to 65536	/Ac/PvOnGrid/L2/Power	no	W
com.victronenergy.system	PV - AC-coupled on input L3	813	uint16	1	0 to 65536	/Ac/PvOnGrid/L3/Power	no	W
com.victronenergy.system	PV - AC-coupled on generator L1	814	uint16	1	0 to 65536	/Ac/PvOnGenset/L1/Power	no	W
com.victronenergy.system	PV - AC-coupled on generator L2	815	uint16	1	0 to 65536	/Ac/PvOnGenset/L2/Power	no	W
com.victronenergy.system	PV - AC-coupled on generator L3	816	uint16	1	0 to 65536	/Ac/PvOnGenset/L3/Power	no	W
com.victronenergy.system	AC Consumption L1	817	uint16	1	0 to 65536	/Ac/Consumption/L1/Power	no	W
com.victronenergy.system	AC Consumption L2	818	uint16	1	0 to 65536	/Ac/Consumption/L2/Power	no	W
com.victronenergy.system	AC Consumption L3	819	uint16	1	0 to 65536	/Ac/Consumption/L3/Power	no	W
com.victronenergy.system	Grid L1	820	int16	1	-32768 to 32767	/Ac/Grid/L1/Power	no	W
com.victronenergy.system	Grid L2	821	int16	1	-32768 to 32767	/Ac/Grid/L2/Power	no	W
com.victronenergy.system	Grid L3	822	int16	1	-32768 to 32767	/Ac/Grid/L3/Power	no	W
com.victronenergy.system	Genset L1	823	int16	1	-32768 to 32767	/Ac/Genset/L1/Power	no	W
com.victronenergy.system	Genset L2	824	int16	1	-32768 to 32767	/Ac/Genset/L2/Power	no	W
com.victronenergy.system	Genset L3	825	int16	1	-32768 to 32767	/Ac/Genset/L3/Power	no	W
com.victronenergy.system	Active input source	826	int16	1	0 to 32768	/Ac/ActiveIn/Source	no	0=Not available;1=Grid
com.victronenergy.system	Battery Voltage (System)	840	uint16	10	0 to 6553.5	/Dc/Battery/Voltage	no	V DC
com.victronenergy.system	Battery Current (System)	841	int16	10	-3276.8 to 3276.7	/Dc/Battery/Current	no	A DC
com.victronenergy.system	Battery Power (System)	842	int16	1	-32768 to 32767	/Dc/Battery/Power	no	W
com.victronenergy.system	Battery State of Charge	843	uint16	1	0 to 100	/Dc/Battery/Soc	no	%
com.victronenergy.system	Battery state (System)	844	uint16	1	0 to 65536	/Dc/Battery/State	no	0=Idle;1=charging;2=dis
com.victronenergy.system	Battery Consumed Amphours (System)	845	uint16	-10	0 to -6553.6	/Dc/Battery/ConsumedAmphours	no	Ah
com.victronenergy.system	Battery Time to Go (System)	846	uint16	0,01	0 to 6553600	/Dc/Battery/TimeToGo	no	s
com.victronenergy.system	PV - DC-coupled power	850	uint16	1	0 to 65536	/Dc/Pv/Power	no	W
com.victronenergy.system	PV - DC-coupled current	851	int16	10	-3276.8 to 3276.7	/Dc/Pv/Current	no	A DC

Figure 30. Data selection

The selection of the relevant data for the project is shown in table 14, where they are accompanied by information on the unit in which they are found and their format.

Table 15. Selected values that will be taken in every sample of the program

General data	Date	DD.MM.YYYY
	Time	HH:MM:SS
	Iteration	
Unit 245: Battery	Ac consumption	Watts
	Grid consumption	Watts
	Battery voltage	Volts
	Battery current	Ampers
	Consumed AmpHours	Ampere hour
	State of charge	%
	Time to go	Hours
Unit 247: Solar Charger	PV voltage	Volts
	PV current	Ampers
	PV power	Watts
Unit 246: Vebus	Input voltage	Volts
	Input current	Ampers
	Input frequency	Hertz
	Input power	Watts
	Output voltage	Volts
	Output current	Ampers
	Output frequency	Hertz
Output power	Watts	

3.1.3 Program development

This section is intended to give a broad outline of how the LabVIEW program works, and the process that has been followed throughout its development, as well as the logical process and a small introduction to the world of programming with block diagrams. Other Labview programs from related published theses (Treviño and Zubieta, 2020); (Benet and Vilella, 2019) used the solution from what looks like a common generic source. The Labview program developed has an improved design that resembles those previously cited, with an equally effective structure, but much simpler since this project is focused on students and it is aimed to be an educational tool.

Once the selection of the information to be acquired from the system has been made, with its registers and to which UnitID they belong, the next step is to design in LabVIEW the block diagram that allows this information to be read through the Modbus connection with the system. In other words, what the Qmodmaster did but in LabVIEW so that the information obtained can be processed later. Figure 31 shows the components of what will be the basic block diagram from which the system information will be obtained.

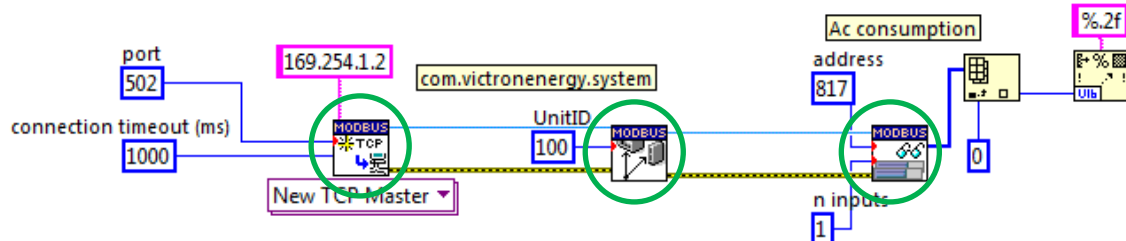


Figure 31. Modbus TCP data collection block diagram

The diagram may seem complex at first sight but each block will be explained in detail what it does, to understand how it works as a group. In the diagram, there are three main blocks circled in green.

The first block is called “Create Modbus instance” which allows us to create an instance as Master that will allow us to access the system through a TCP Modbus connection. This block needs the IP address with which it must communicate, in this case, 169.254.1.2, which

corresponds to the Main Unit of the system, provided by Victron Energy. The block also needs information on the port to which it is connected, which is always 502, and the connection timeout, which in the case of this Main Unit is one second. This means that the system updates the information every second, so it will not be possible to carry out analyses where it is necessary to obtain data with a time interval lower than this.

The middle block is in charge of establishing which UnitID is to be accessed to get the information from its registers. In our system, there are only 4 units, but if more solar panels, batteries or other equipment were used, this number would increase. The registers to be read are in units 100 (system), 245 (battery), 246 (vebus), 247 (solar charger).

The third block "Read Input Registers" is the one that accesses the information in the register that it is assigned to, in the image it is 817. This block also has the option of reading a few registers in a row without the need for more blocks, but because of the numbers of the registers that need to be read, this will not be used. This block accesses the register that has been set and returns the information that is in that register in array format, the following blocks are only to change the format in which the information is written to be able to write it in a spreadsheet.

The three main blocks are interconnected with two connections as shown in Figure 31, the top one is the TCP master instance that shares the information that has been entered into each of the blocks (IP address, port, connection timeout, UnitID, etc.) and the bottom one is the error signal. Its function is to activate the next block when it receives the impulse from the previous block. These blocks described belong to the external LabVIEW library: LabVIEW Modbus API.

The Modbus TCP data collection block diagram will be repeated for each of the data to be collected at the same instant in time, a small summary of the appearance of this part of the program can be seen in Figure 32.

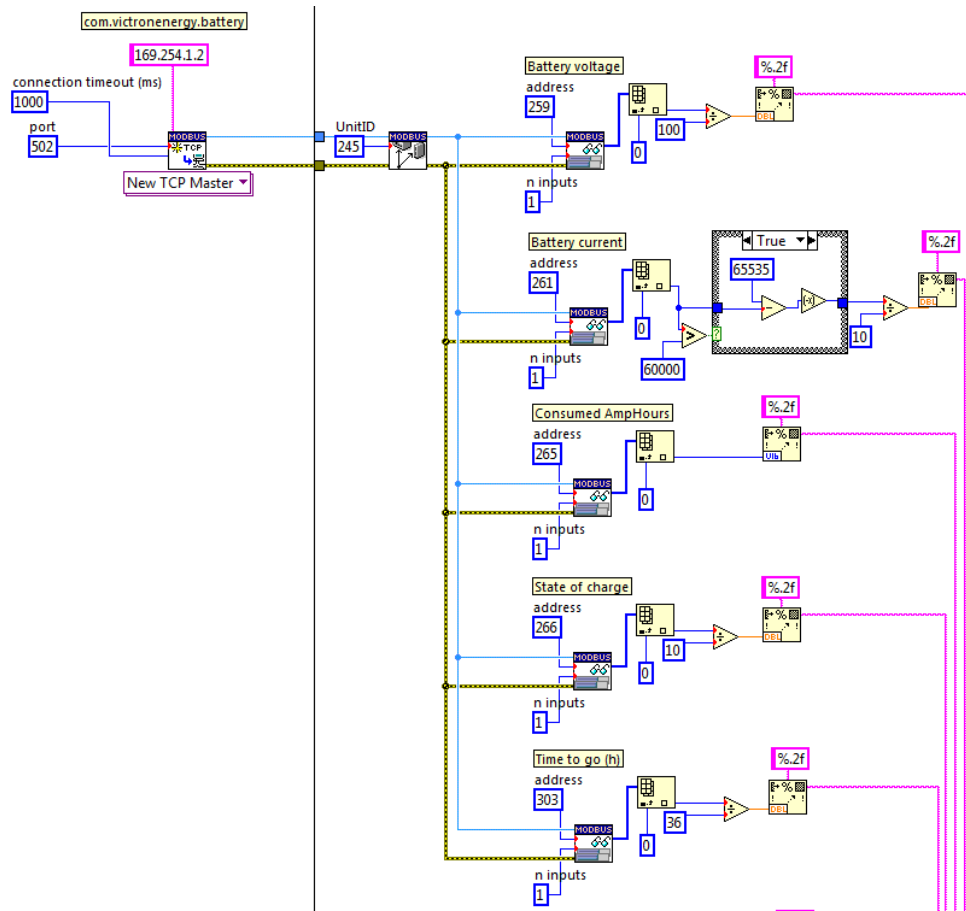


Figure 32. Data collection summary in LabVIEW

Figure 32 is a small portion of the final block diagram of the entire program as a whole, which can be found in Appendix II, but Figure 32 gives a closer look at the work behind the designed program. For the creation of a spreadsheet to store all the information collected from each of the records relevant to the project as described above, the following block diagram (Figure 33) will be used.

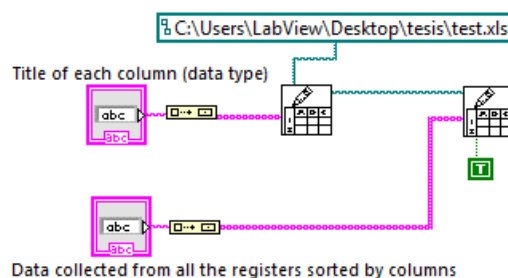


Figure 33. Creation of a spreadsheet with the data block diagram

In Figure 33, there are two blocks designated to create spreadsheets. As they are interconnected with each other they will share settings as well as the location where they are placed and by ticking the "append to file" box in the second one, the file will not be replaced but will be written one row below the other. Thus, it was decided that the first block would contain the titles of the data to be collected and the second block would contain the data to be appended so that if you want to add more data, you only have to activate the second block again.

Knowing these two things, it is easy to follow the next steps, which will be to repeat the first block diagram to obtain the data from each of the system's registers, concatenate all the results in an array and put this in the second block of the second block diagram.

Since what is desired is a continuous analysis of the data collected, it must be built into the program to continuously take data and add it to the spreadsheet, and now comes into play what in programming is called a *for loop*. A loop is a sequence of instructions that is executed repeatedly until the condition assigned to the loop is no longer satisfied. For example, to take data *for* 30 seconds, and adding a 2-second delay to this *for loop* then the system will take data every 2 seconds for 30 seconds, so 15 samples in total.

The block diagram of the final program developed with LabVIEW can be found in Appendix II.

3.2 Designing LabVIEW Interface

LabView is a robust program and can sometimes be difficult to understand for non-programmers or students without prior knowledge of the program. For this reason, a good, intuitive, coherent and interactive interface is required.

The interface plays a fundamental role and makes the product competitive or not (LaCalle, 2021). Figure 34 shows the interface created for the developed program explained in section 3.1.3 *Developing LabVIEW*.

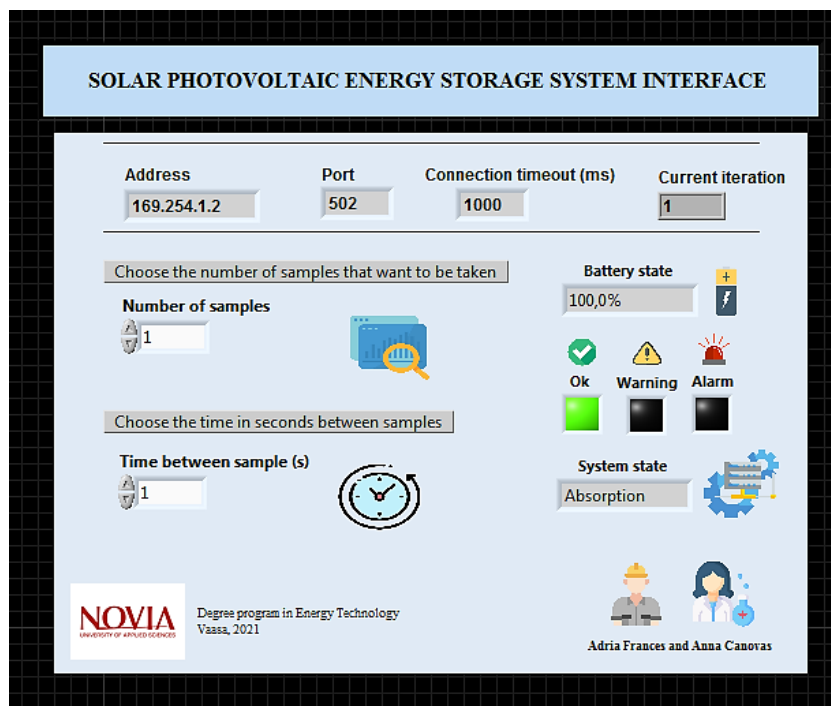


Figure 34. Final Interface of the project

The top part between the lines gives the user information about the IP address of the system which identifies the device with the ability to connect to the internet in the case at some point the student wishes to connect or add another type of device to the system. The port, to which it is connected, and the connection timeout, which indicates that the system is updating the information every second. Lastly, there is the number of the current iteration. The user can view in real-time how the number of iterations increases as the system collects the data in Excel. This part is purely informative and the student cannot make any adjustments.

Afterwards, two values can be set by the user: the number of samples to be collected and the time to be left between each sample. For each sample, the data specified, and previously chosen, in section 3.1.2. *Data selection* will be collected. As far as the unit of the time between samples was chosen in seconds as it is the one established by the International System of Units. One example that could be mentioned, to have a better understanding, is the one to carry out the analysis of the different scenarios that will be discussed in section 3.3.1 *PV panel analysis*, the number of samples was set in 72, to take one sample every 20 minutes for 24h (one whole day). So, logically, the time between samples was set to 1200 seconds (20 minutes). Each value to be set by the user is accompanied by a brief explanation to achieve a clear and simple interface.

On the right side of the screen, the battery and system status are displayed interactively and attractively because several studies have shown that interactive media enable faster learning for students and facilitate a better attitude towards the assimilation of new content and the acquisition of skills (Milrad, 1999). In addition, coloured lights and sounds on the battery status have also been used for a more professional interface.

Since the design of the interface is student-centered, as well as including nice and user-friendly features, the visual appeal has to be taken into account. For this reason, the same range of colours and design has been used, as in the rest of the project. Also, to make the user feel familiar with some elements, icons have been added to make it easier to understand what is being visualised.

4 Results: Testing the final system

This section will analyse the project under various conditions to ensure full functionality for the educative system. In this way, students will be able to use this educational tool knowing that the data obtained is correct and accurate.

The battery and the photovoltaic panel are the ones that would change the overall efficiency of the system the most, therefore they will be inspected with different tests and possible alternatives available in the present market will be investigated.

The solar panel will be tested in three different scenarios: sunny, cloudy and rainy to prove its efficiency and find possible improvements with the results obtained. Regarding the battery, it will be subjected to a discharge and a full charge to compare the graphs achieved with other types of batteries previously explained in section 2.3 *Batteries*.

4.1 PV panel analysis

As it has been observed there are several types of photovoltaic solar panels and depending on their characteristics, voltage, size, material, efficiency, etc. the performance of the solar panel will vary. To carry out this analysis, the same type of solar panel shown in section 2.4.5 *PV Solar Panel NM35WFL*, a thin-film solar photovoltaic panel, has been used and placed in the same place, direction and angle. The location was Palosaarentie 81, 65230 Vaasa (Finland) (63.11544, 21.6099) with an orientation of 138°SE.

In all three scenarios, the same number of samples were taken and during the same periods to be more accurate and to compare the results under the same conditions. The samples were taken throughout the whole day (24 hours) every 20 minutes. The results obtained on how the voltage varies during the day are shown in the figures of each section. The data will be compared with the meteorological situation at Meteorita Söderfjärden which is located 15km away from where measurements are taken, in Marenintie 292, 65410 Vaasa (63.00845, 21.56836).

Meteorita Söderfjärden is a visiting centre in the middle of a meteorite crater in Finland (Meteorita.fi, 2021) which was visited previously because apart from being a museum, it is an energy cellar, it has its own production of renewable energy: solar and wind. Therefore,

on its website: http://iot.novia.fi/data/meteoria_weather.html all meteorological and energy data collected daily are available.

From the whole range of data offered by Meteoira, the following have been chosen to analyse the operation of the system: the altitude of the sun concerning the horizon, to validate the hours of sunshine detected by the photovoltaic panel, the atmospheric pressure, to justify meteorological changes, the relative humidity, which will confirm the cases in which measurements are taken on rainy days, and finally the solar irradiation, which is the most important factor because it is the determining element for the collection of photovoltaic solar energy.

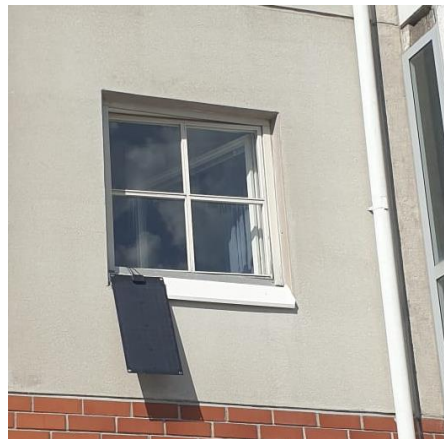


Figure 35. Location of the PV panel

4.1.1 Scenario 1: Sunny weather

The first scenario is the sunny scenario that took place on the 3rd of May 2021. The average temperature that day was 4°C, humidity 59%, pressure 1011mbar and the wind 10,6808511km/h (Custom Weather, 2021). The results obtained on how the voltage varies during the day can be found in: <https://yhnovia-my.sharepoint.com/>, but also there is a brief analysis shown in Figure 36.

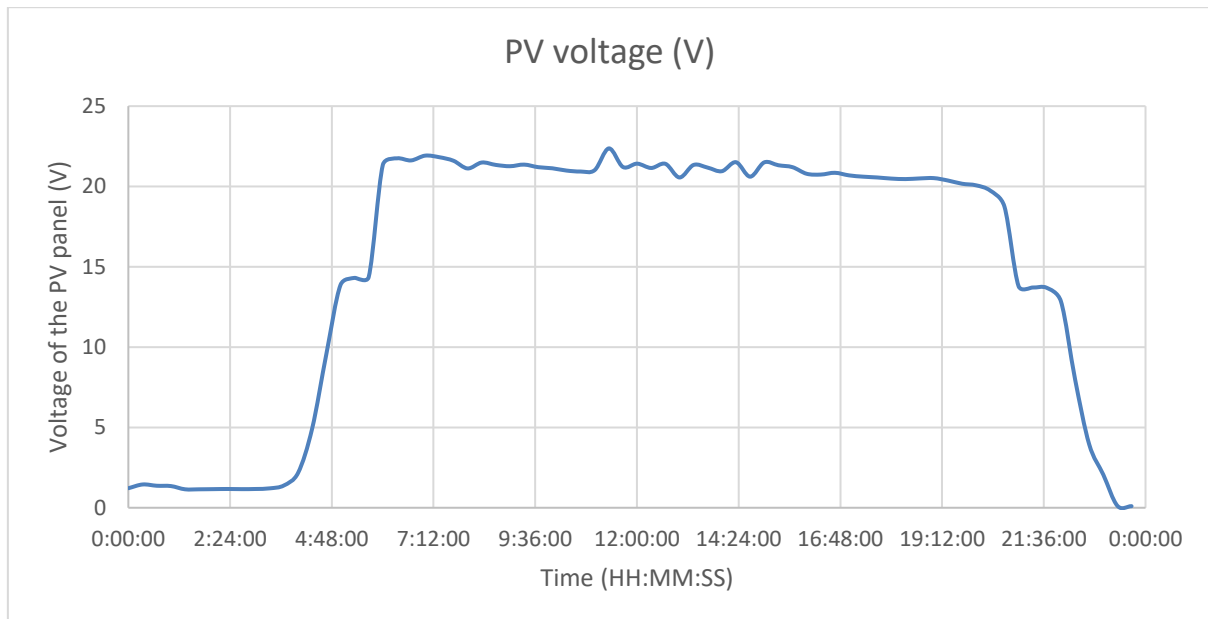


Figure 36. PV Voltage (V) in sunny weather

The figure shows the voltage on the solar panel due to the impact of the sun's radiation on it, taking into account the location of the panel and the orientation, it can be deduced that it has a much greater impact in the morning hours. It can also be seen that on a sunny day, from the time the sun is on the panel until it stops reaching the panel (from 6 am till 9 pm), supported in Figure 37, the voltage is more or less stable at 21-22 volts with some variations probably due to small clouds, or some other distortion.

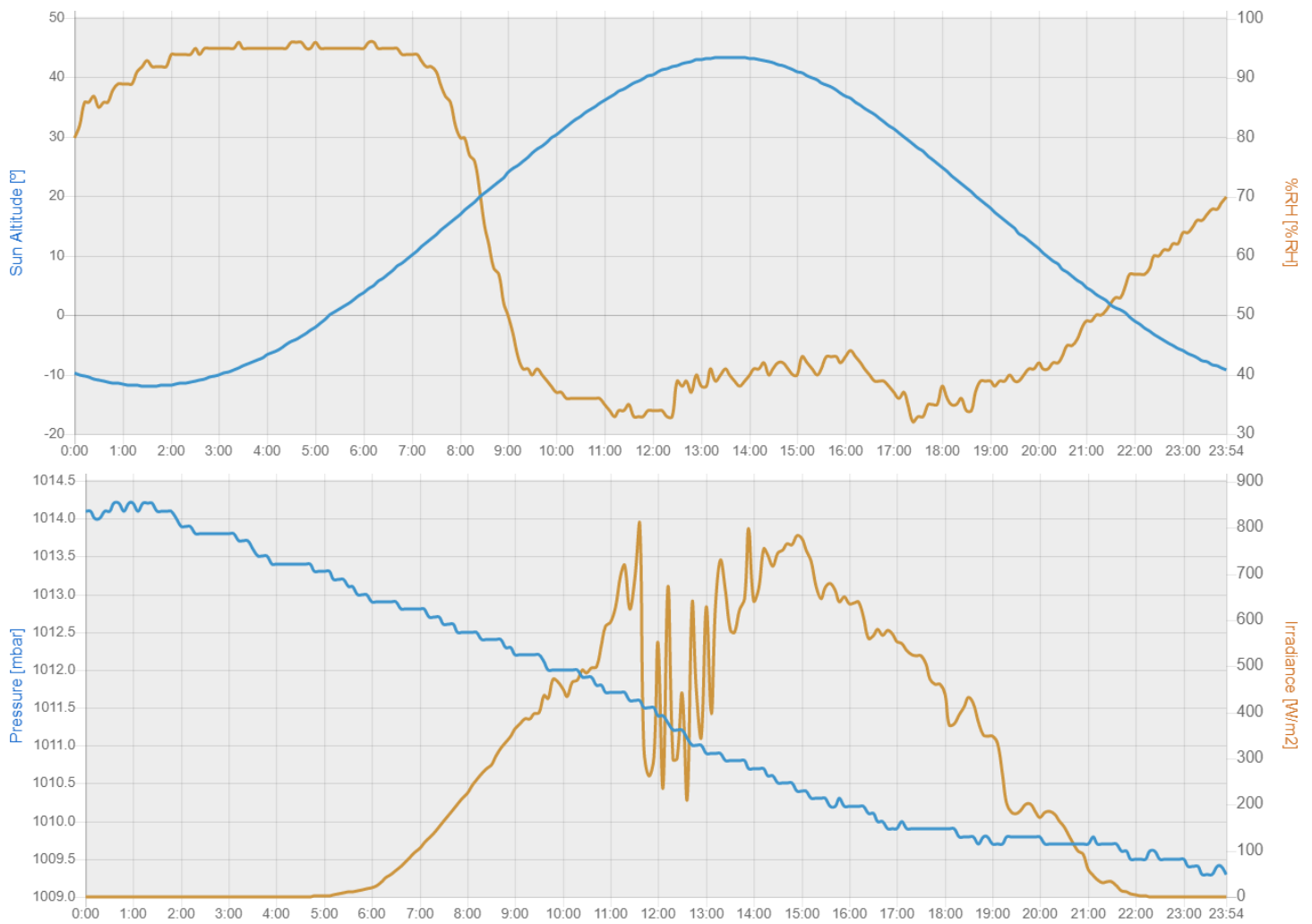


Figure 37. Meteorological data from 3th May (Novia.fi, 2021)

Comparing with the meteorological data extracted from Meteorica Söderfjärden shows that the 3rd of May was a completely sunny day with high solar irradiation, which is very relevant because it determines the amount of solar energy that can be obtained by the photovoltaic panel.

4.1.2 Scenario 2: Cloudy weather

The first scenario is the sunny scenario that took place on the 7th of May 2021. The average temperature that day was 0°C, humidity 69%, pressure 1001mbar and the wind 12,64km/h (Custom Weather, 2021). Samples were taken in the same format as in the first scenario, so that differences in the solar collection could be seen. The data taken of the analysis can be found in: <https://yhnovia-my.sharepoint.com/>, but also there is a brief analysis shown in Figure 38.

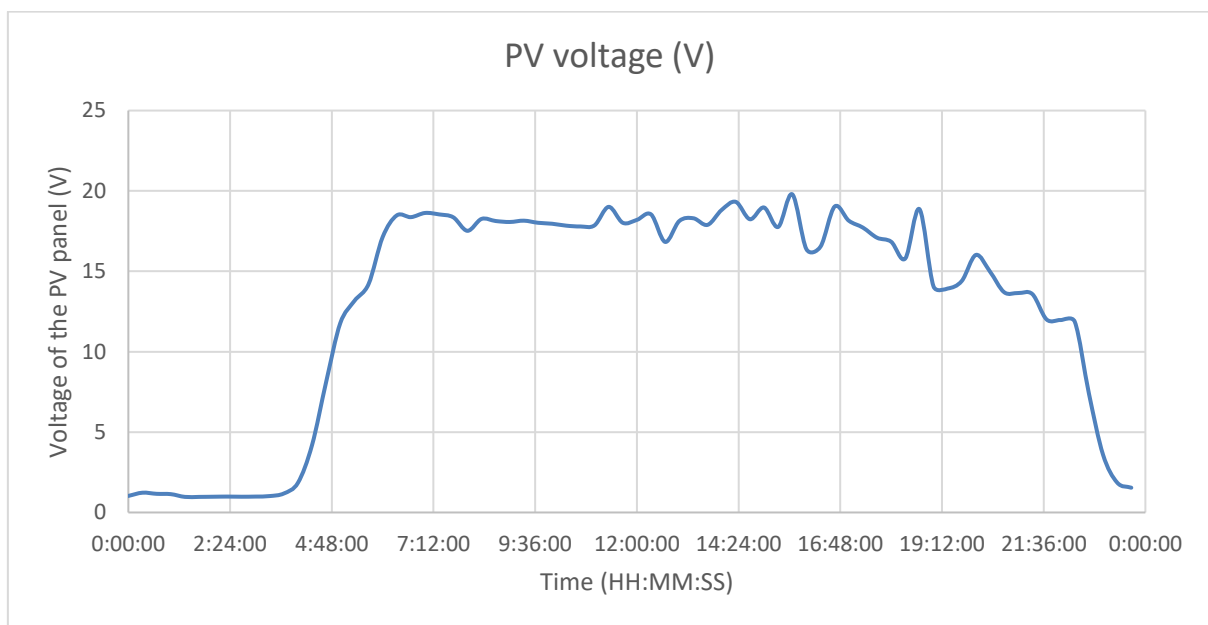


Figure 38. PV Voltage (V) in cloudy weather

The figure shows, as in the previous case, the voltage on the solar panel due to the impact of solar radiation on it, it can be seen that during the same hours as in the previous case (from 6 am to 9 pm) there is an increase and a stabilisation of the solar gain. In this case of a cloudy day, can be seen that this stabilisation occurs around 17-18 volts, a value significantly below that of scenario 1. It can also be seen that during the afternoon, there are considerably more oscillations than in the morning because at some moments the sun came out and this is the factor that distorts the graph a little. The conclusion is that the average voltage value obtained during sunny hours is 15% lower than in the previous scenario.

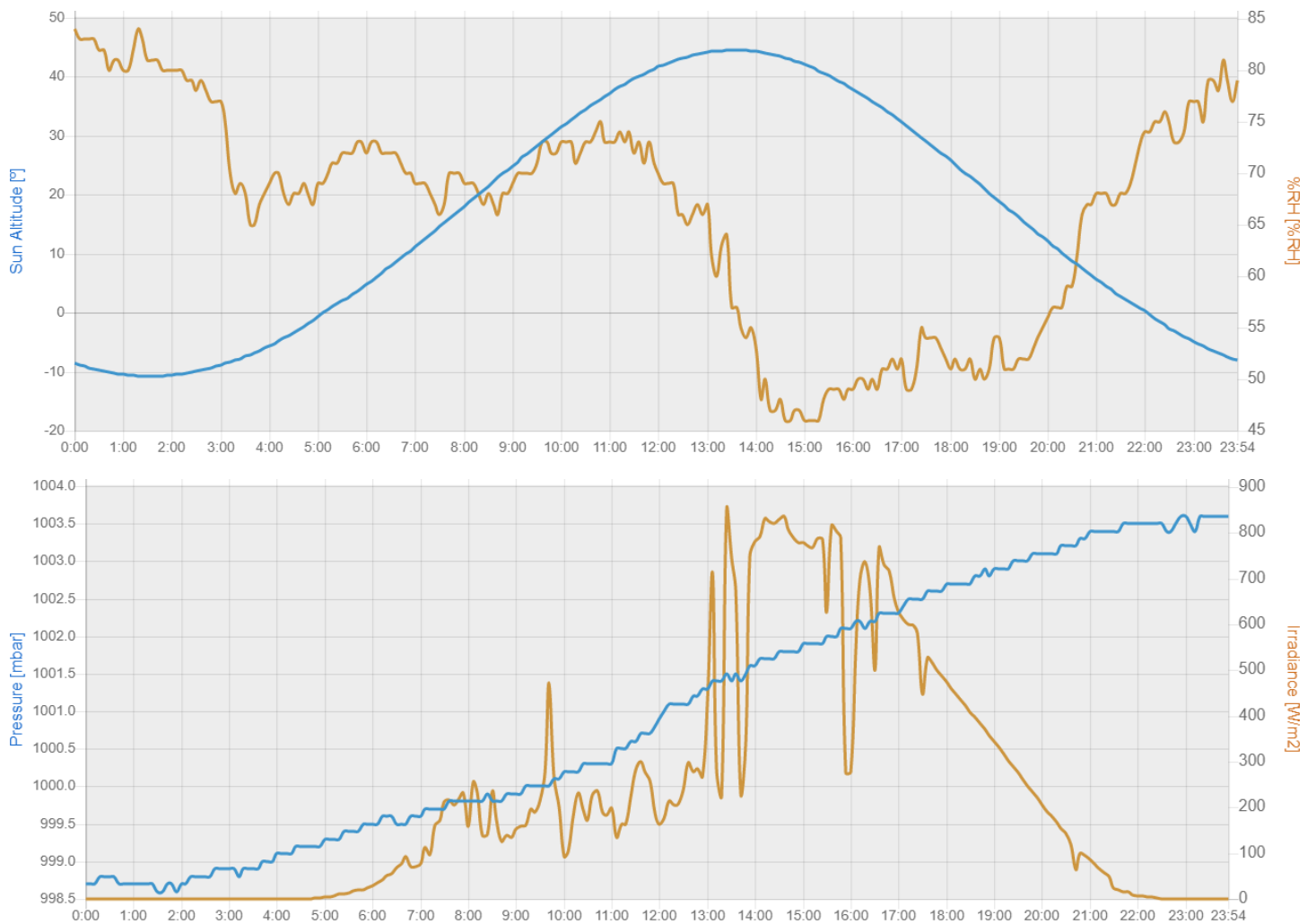


Figure 39. Meteorological data from 7th May (Novia.fi, 2021)

Figure 39 shows that the altitude of the sun is the same as in scenario 1, the humidity is considerably higher, the pressure is lower, but the relevant data is the solar irradiance, which, although cloudy, is still quite high compared to the other day. This explains that even if it is cloudy, the solar panel is still producing solar energy.

4.1.3 Scenario 3: Rainy weather

The last scenario is the one with rainy weather that took place on the 10th of May 2021. The average temperature that day was 0°C, humidity 90%, pressure 1010mbar and the wind 12,36km/h (Custom Weather, 2021). Samples were taken in the same format as in the first and second scenarios, so that differences in the solar collection could be seen. The obtained results can be observed in: <https://yhnovia-my.sharepoint.com/>, in Figure 40 there is a brief analysis.

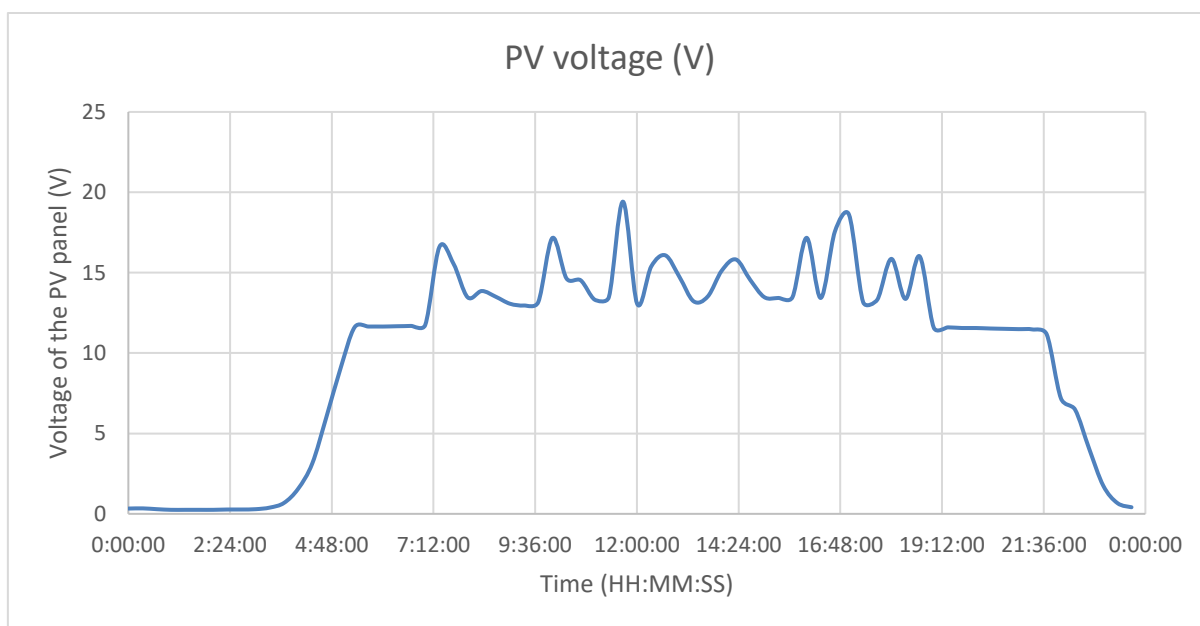


Figure 40. PV Voltage (V) in rainy weather

The figure shows, as in the previous cases, the voltage on the solar panel due to the solar impact on it, as in the other cases, it can be seen that during the same hours (from 6 to 21 hours) there is an increase in solar gain. In this case, unlike the others, it is not so stable during the hours of sunlight, there are quite a few peaks and the voltage rises and falls caused by rain. With the calculation of the average voltage it can be seen that this stabilisation occurs at around 13-14 volts, a value sensibly lower than that of scenario 2 and notably lower than that of scenario 1, which in percentage terms can be summarised as a decrease of 40%.

Unfortunately, for reasons beyond our control, and as can be seen in Figure 41, Meteoris Söderfjärden did not publish data from 6 a.m. on 10 May until 4 a.m. on 11 May. Therefore,

there is no meteorological data to corroborate in detail what was analysed on that day. The only thing that can be said about that day is that it rained between the hours for which there is no data because the following day there was accumulated rain that had not been counted the day before.

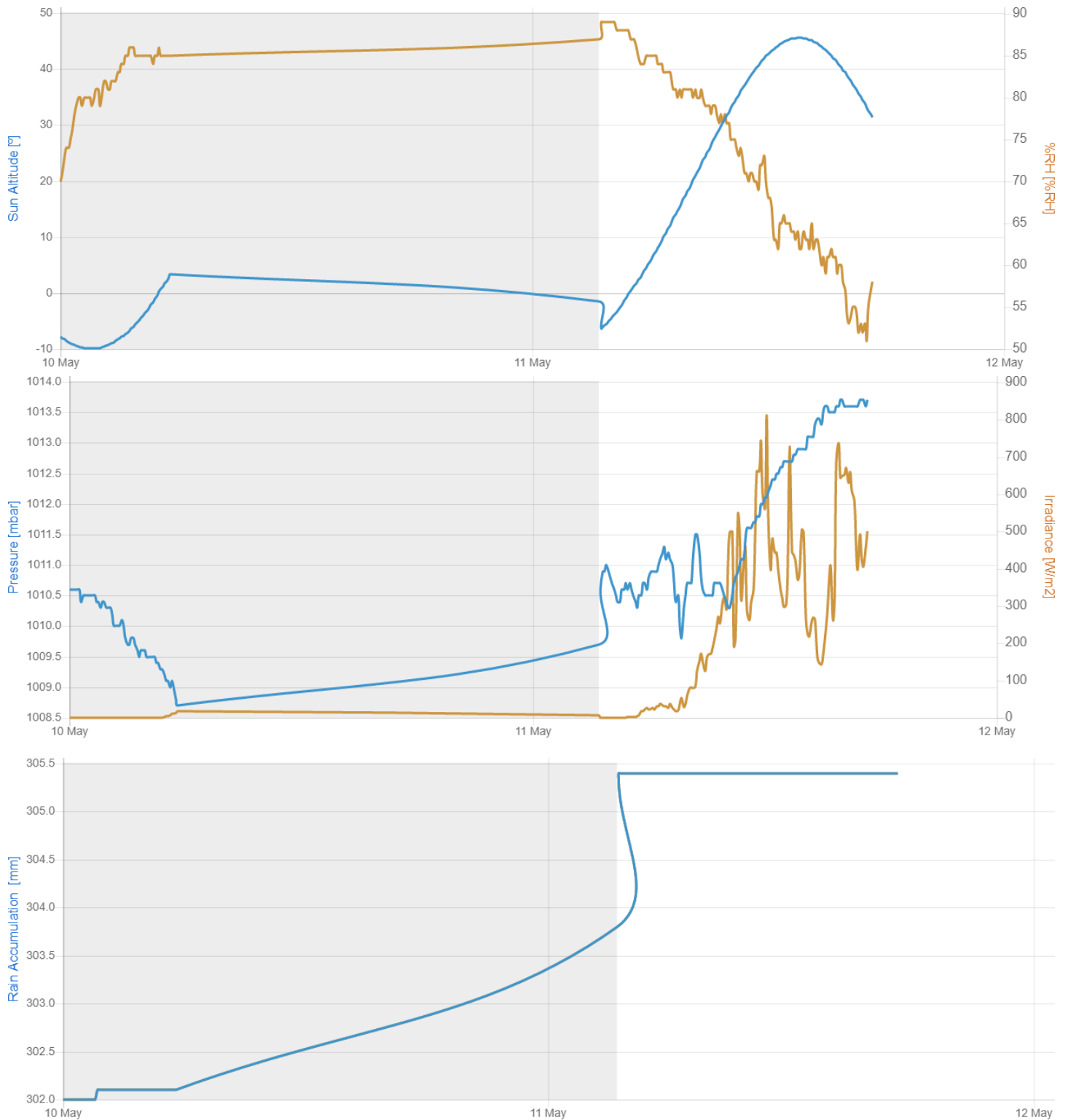


Figure 41. Meteorological data from 10th of May (Novia.fi, 2021)

4.1.4 PV panel possible alternatives

Different solar panels have been considered for implementation in the system, such as a monocrystalline panel. Although it has not been possible to carry out practical tests with this type of panel due to lack of availability, has been reported in the theoretical part to have much higher efficiency. This is further corroborated in many scientific tests (Cotfas and Cotfas, 2019).

The use of a crystalline panel would improve the efficiency of the system and therefore increase the sustainability of the installation as well. But the key feature that has made the thin-film panel option the best choice is that, as the project is focused on educational purposes, a panel that is lightweight and portable can provide the project with many different study opportunities, one of them being that this type of PV panel can be moved to different locations easily.

4.2 Battery analysis

The AGM 51Ah battery will also be analysed as it discharges to prove its correct functioning and to compare it with other batteries of different types according to their chemical composition to see possible alternatives available. As only the above battery is physically available, discharge data shall be collected from the real discharge of the battery and compared with discharge graphs of other batteries provided by the manufacturer.

4.2.1 Discharge

The analysis will focus only on the discharge of the battery when a constant load of 102W is applied. This is one of the main factors an engineer should take into account when specifying a battery to match the performance requirements of the end product (Mpoweruk, 2021). Samples of the voltage of the battery at each point in time and the discharge current will be taken every 30 seconds to see how the discharge evolves, and the study will last until the battery is discharged (10% margin because otherwise it will be damaged). As a consequence, a very high number of samples will be taken to stop collecting data manually and start charging the battery when the alarms turn on since the discharge time is uncertain. The data extracted from the discharge can be observed in <https://yhnovia-my.sharepoint.com/> and the battery voltage and current during the discharge can be seen in Figure 42.

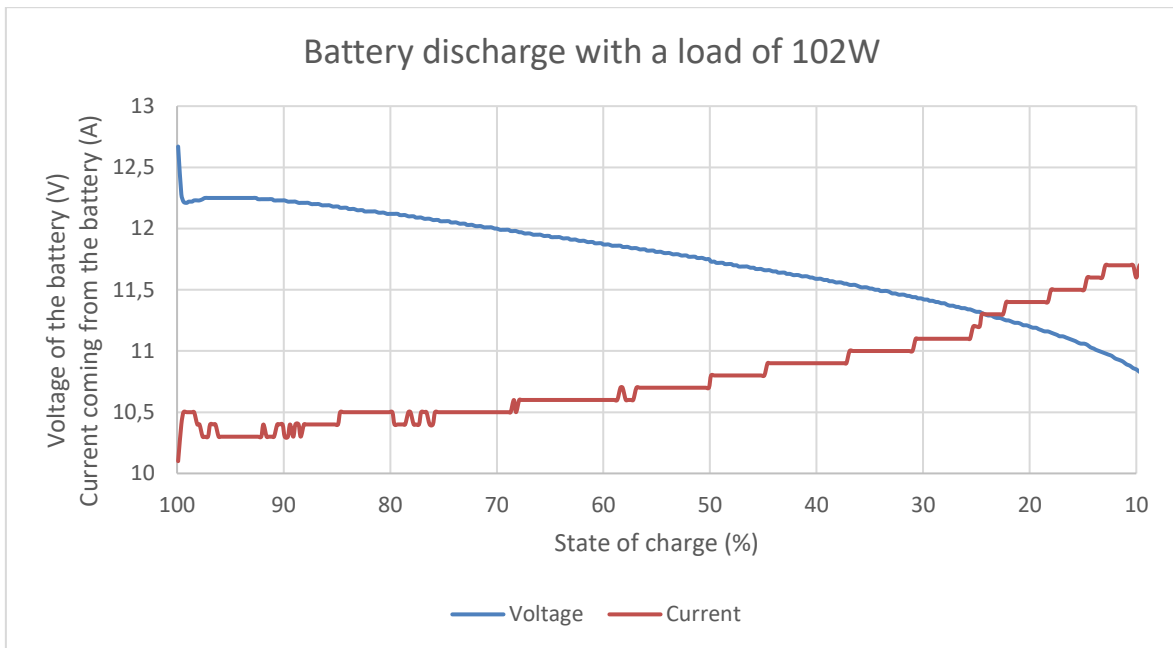


Figure 42. AGM 51Ah battery discharge

The first conclusions that can be drawn from the data are that when the battery is discharging the voltage is reduced, this increases the current because $P=V \cdot I$ and because a constant power of 102W must be supplied. This explains that the product of both curves must be 102W all the time, which is why they appear symmetrical to each other, neglecting small variations.

4.2.2 Battery possible alternatives

Different types of batteries are going to be compared with the AGM battery involved in the project. Comparing the discharge curves of a Li-ion battery, one of the most popular types of battery currently in the market, it can be observed that the curves are quite similar (Figure 43 and 44).

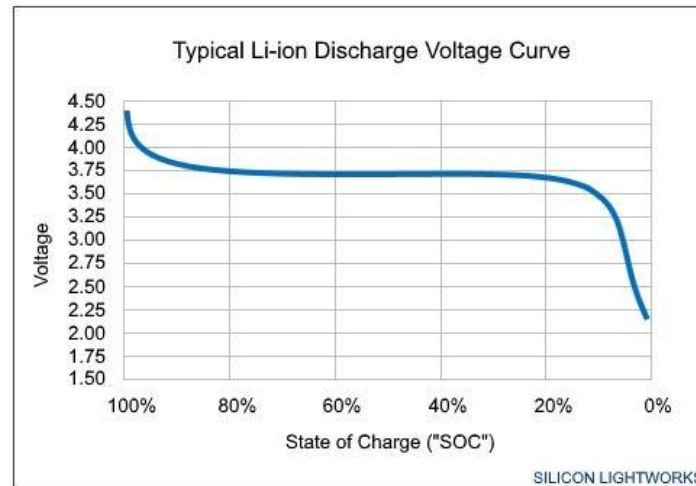


Figure 43. Typical Li-ion discharge voltage curve (Silicon Lightworks, 2016)

In the curve can be appreciated that in the Li-ion battery, the discharge voltage is more or less constant from 80% to 20% charge and in AGM the voltage continuously decreases but it is not from 20% that the drop is more pronounced. This battery would provide a more constant output current on the system.

In the following, different types of deep cycle batteries such as Lead Acid or Gel batteries with AGM batteries will be compared, as they have similar discharge curves with small differences. It should be mentioned that the curves are created with typical values of these batteries in the state of discharge.

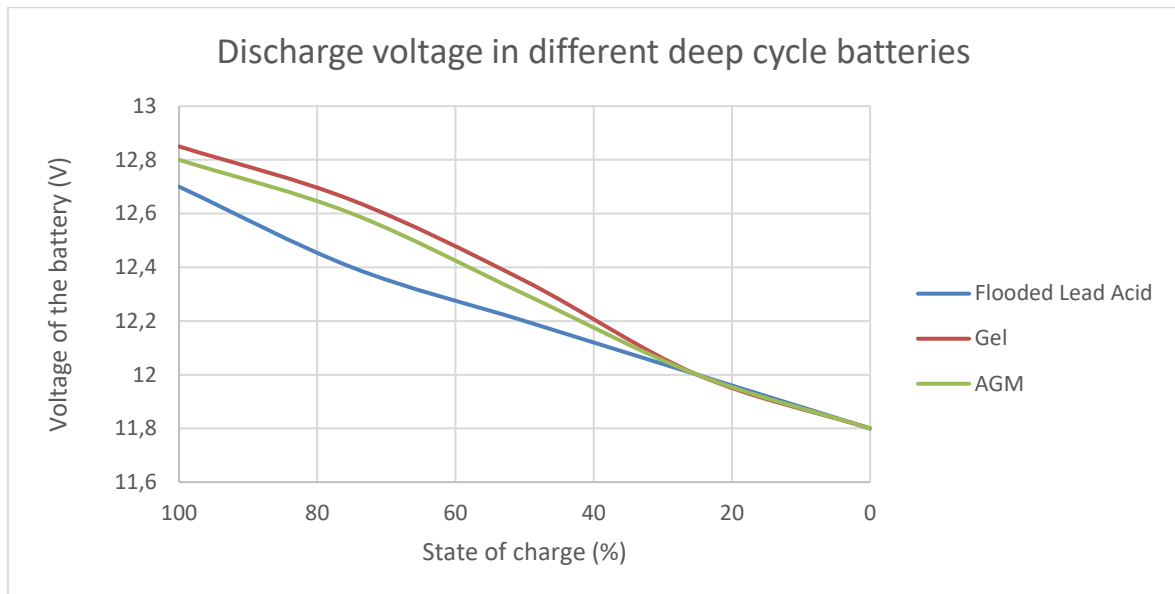


Figure 44. Discharge voltage in different deep cycle batteries -Adapted from (don, 2016)

The differences between Gel and AGM batteries are minimal and no conclusions can be drawn, but concerning the Flooded Lead Acid battery, it is clear that its curve is quite different from that of the utilised battery. The discharge is much more sloped, almost in a straight line. This with a battery should be avoided as much as possible because it means that the battery is not supplying the same voltage all the time, but is constantly fluctuating, and therefore, with a constant load, the current is also constantly increasing.

5 Discussion

Concerning the original thesis aims and objectives

The first objective was performed through the development of the system software using the LabVIEW program which could collect data to an Excel sheet from four different units - system, vebus, solar charger and battery.

Referring to the second objective an intuitive, interactive and user-friendly interface was designed meticulously allowing the students to carry out -in an easy way- an analysis of the system.

The performance of the different test, allowed us to meet the third objective, the insurance of the proper functioning through the collection of solar energy with the photovoltaic panel in three different scenarios by changing its meteorological conditions and the discharging AGM battery test with a constant load of 102W. As expected, it was determined that the most optimum outcome (which gave the best data and therefore the highest voltage), was with the sunny weather, secondly the cloudy and finally the rainy weather. In addition, the curve obtained from the discharge of the battery was quite symmetrical, disregarding small variations, which verifies its good performance as the load was constant.

Concerning the limitations of the work

As there was no prior knowledge of LabVIEW, this part of the project became complex and crucial, making the programming in the block diagram process longer than expected. Regarding the analysis made on PV panels, it would have been useful to test it over more days to average it and obtain more conclusive data without generalizing. This could not be done as the equipment was not available until the beginning of April when it was originally scheduled for delivery in mid-January.

Normally the interfaces of technological tools that collect and analyse data are cumbersome and unattractive, so it was necessary to think about how to make it easy to use and engaging for students without prior examples of designs.

It must also be mentioned that the undertaken test to prove the proper functioning of the battery in discharge conditions had to be with a margin of a 10% in the state of charge because otherwise it would have been damaged.

Concerning the consistencies

The developed educational tool will be important and very useful for the learning methods used in the education sector in Finland and Europe with the increase of renewable energy projects.

Moreover, the LabVIEW part of the project provided an insight into an important and wide-ranging program that is used by millions of engineers and scientists to develop sophisticated testing and control applications, which aroused and sparked great interest because of the possibilities it offers, in addition to contributing to the completion of the other objectives. The section 4.1 PV Panel analysis confirmed that the system in use was working properly and efficiently like the AGM 51h battery and the section 4.2 Battery analysis gave new insight on the batteries to be used as if the project were to go to a larger scale, Li-ion batteries should be taken into account according to Podder and Khan, (2016).

6 Conclusions

As technology is constantly evolving, it is important to continue to research all the possibilities available to make the most of the renewable energies that are currently on the rise, which has led the European Union to promote more energy efficiency projects. Based on the fact that technological tools are very important in Finland and their use in education is being encouraged, the project will address the following challenges: the generation and storage of clean energies, creating an educational tool that will allow quantitative studies of these energies.

During all the tests performed, the system operated correctly and no anomalies were detected, apart from a few deviating data, even though the global result was not altered. As well, these results corroborated the information extracted from the previous research on batteries and photovoltaic panels and remarked that those used were the best choices for a project of this scale.

The Solar Photovoltaic Energy Storage System has many interesting applications and therefore with the evolution of technology many of them could be implemented in further projects. A very important step forward in this project would be the implementation of an application for smartphones, which could take remote control of the system and thus collect data in real-time for future analysis and due to the pandemic situation, where it is sometimes required to work abroad.

This project has allowed us to enter the world of renewable energy storage, specifically photovoltaic solar energy, such as to deepen and improve both the theoretical knowledge of the chemical reactions that are continuously produced in the system and the practical knowledge of the programming of the block diagrams.

7 List of references

Akkupojat.fi. (2021). *Taipuisat yksikidepaneelit*. [online] Available at:

https://www.akkupojat.fi/tuotteet/aurinkopaneelit-ja-tarvikkeet/aurinkopaneelit/aurinkopaneelit-_682445/taipuisat-yksikidepaneelit-_626501 [Accessed 9 May 2021].

Analog. (2017). *Chapter 5: Solid-state diodes and diode characteristics [Analog Devices Wiki]*. [online] Available at:

<https://wiki.analog.com/university/courses/electronics/text/chapter-5> [Accessed 6 May 2021].

Andres (2017). *Cual es el mejor tipo de panel solar – Mono/Polycrystalline/Thin Film?*

[online] Electricaplicada. Available at: <https://www.electricaplicada.com/cual-es-el-mejor-tipo-de-panel-solar-mono-polycrystalline-thin-film/#paneles-solares-string-ribbon> [Accessed 29 Apr. 2021].

Aurinkopaneelikauppa. (2021). *AGM Battery 51Ah*. [online] Available at:

https://www.aurinkopaneelikauppa.fi/epages/aurinkopaneelikauppa.sf/en_GB/?ObjectPath=/Shops/20120903-11092-142553-1/Products/%2205051%206%22 [Accessed 29 Apr. 2021].

Basic Electronics Tutorials. (2013). *PN Junction Theory for Semiconductor Diodes*.

[online] Available at: https://www.electronics-tutorials.ws/diode/diode_2.html [Accessed 6 May 2021].

Batteryuniversity. (2011). *Advantages & Limitations of the Lithium-ion Battery - Battery University*. [online] Available at:

https://batteryuniversity.com/learn/archive/is_lithium_ion_the_ideal_battery [Accessed 6 May 2021].

Batteryuniversity. (2016). *Sulfation and How to Prevent it - Battery University*. [online]

Available at: https://batteryuniversity.com/learn/article/sulfation_and_how_to_prevent_it [Accessed 6 May 2021].

Batteryuniversity. (2018). *Lead-based Batteries Information – Battery University*. [online]

Available at: https://batteryuniversity.com/learn/article/lead_based_batteries [Accessed 6 May 2021].

Batteryuniversity. (2019). *Types of Lithium-ion Batteries – Battery University*. [online] Available at: https://batteryuniversity.com/learn/article/types_of_lithium_ion [Accessed 6 May 2021].

Battery University. (2020). *Absorbent Glass Mat (AGM) Battery Information - Battery University*. [online] Available at: https://batteryuniversity.com/learn/article/absorbent_glass_mat_agm [Accessed 29 Apr. 2021].

Benet, A. and Vilella, A. (2019). Comparison of Solar Thermal and Photovoltaic Panels. *Theseus.fi*. [online] Available at: <https://www.theseus.fi/handle/10024/226622> [Accessed 19 May 2021].

Brain, M (2021). *How Lithium-ion Batteries Work*. [online] HowStuffWorks. Available at: <https://electronics.howstuffworks.com/everyday-tech/lithium-ion-battery.htm> [Accessed 6 May 2021].

Britannica. (2021). In: *Encyclopædia Britannica*. [online] Available at: <https://www.britannica.com/science/silicon> [Accessed 11 May 2021].

Bowden,S. and Honsberg,C. (2021). *Formation of a PN-Junction / PVEducation*. [online] Available at: <https://www.pveducation.org/pvcdrom/pn-junctions/formation-of-a-pn-junction> [Accessed 6 May 2021].

Bowden, S and Honsberg, C (2021). *Operation of Lead Acid Batteries / PVEducation*. [online] Available at: <https://www.pveducation.org/pvcdrom/lead-acid-batteries/operation-of-lead-acid-batteries> [Accessed 6 May 2021].

CCE Finland OY. (2021). [online] Available at: <https://www.ccefinland.org/information-comm-technology> [Accessed 12 May 2021].

Chemistry LibreTexts. (2013). *Oxidation-Reduction Reactions*. [online] Available at: [https://chem.libretexts.org/Bookshelves/Analytical_Chemistry/Supplemental_Modules_\(Analytical_Chemistry\)/Electrochemistry/Redox_Chemistry/Oxidation-Reduction_Reactions](https://chem.libretexts.org/Bookshelves/Analytical_Chemistry/Supplemental_Modules_(Analytical_Chemistry)/Electrochemistry/Redox_Chemistry/Oxidation-Reduction_Reactions) [Accessed 4 May 2021].

Chemistry LibreTexts. (2015). *17.5: Batteries and Fuel Cells*. [online] Available at: [https://chem.libretexts.org/Bookshelves/General_Chemistry/Chemistry_\(OpenSTAX\)/17%3A_Electrochemistry/17.5%3A_Batteries_and_Fuel_Cells](https://chem.libretexts.org/Bookshelves/General_Chemistry/Chemistry_(OpenSTAX)/17%3A_Electrochemistry/17.5%3A_Batteries_and_Fuel_Cells) [Accessed 4 May 2021].

Doerffel, T. (2021). *QModBus homepage*. [online] Sourceforge.net. Available at: <http://qmodbus.sourceforge.net/> [Accessed 28 Apr. 2021].

don (2016). *Deep cycle battery voltage & state of charge*. [online] Energy Matters. Available at: <https://www.energymatters.com.au/components/battery-voltage-discharge/> [Accessed 7 May 2021].

Earth Science Communications Team. (2021). *Climate Change Evidence: How Do We Know?* [online] Available at: <https://climate.nasa.gov/evidence/> [Accessed 17 May 2021].

Enerdata.net. (2020). *World Power consumption | Electricity consumption | Enerdata*. [online] Available at: <https://yearbook.enerdata.net/electricity/electricity-domestic-consumption-data.html> [Accessed 3 Nov. 2020].

EnergySage (2020). *Types of thin-film solar panels*. [online] Solar News. Available at: <https://news.energysage.com/types-of-thin-film-solar-panels/> [Accessed 29 Apr. 2021].

EnergySage. (2021). *Monocrystalline vs. Polycrystalline Solar Panels | EnergySage*. [online] Available at: <https://www.energysage.com/solar/101/monocrystalline-vs-polycrystalline-solar-panels/> [Accessed 29 Apr. 2021].

Farrell, C., Marsh, J. and Bertrand, M. (2019). *Are We Motivating Students with Data?* [online] . Available at: <https://cdn2.hubspot.net/hubfs/6485347/Blog%20Assets/Are%20We%20Motivating%20Students%20with%20Data.pdf>. [Accessed 13 May 2021].

Fsu.edu. (2021). *Molecular Expressions: Electricity and Magnetism: Alkaline Battery*. [online] Available at: <https://micro.magnet.fsu.edu/electromag/electricity/batteries/alkaline.html> [Accessed 4 May 2021].

Glenergy Solar. (2015). *Solar PV Panels in Ireland - Glenergy Solar*. [online] Available at: <http://glenergysolar.ie/solar-pv/solar-panels-ireland-how-does-solar-pv-work/> [Accessed 11 May 2021].

Gsu.edu. (2021). *Batteries*. [online] Available at: <http://hyperphysics.phy-astr.gsu.edu/hbase/electric/battery.html> [Accessed 4 May 2021].

- Gsu.edu. (2021). *The P-N Junction*. [online] Available at: <http://hyperphysics.phy-astr.gsu.edu/hbase/Solids/pnjun.html> [Accessed 6 May 2021].
- InfoClutch. (2021). *List of Companies Using LabVIEW, Market Share and Customers List*. [online] Available at: <https://www.infoclutch.com/installed-base/cad-software/labview/> [Accessed 11 May 2021].
- Jäger-Waldau, A. (2020). Snapshot of Photovoltaics—February 2020. *Energies*, [online] 13(4), p.930. Available at: <https://www.mdpi.com/1996-1073/13/4/930/htm> [Accessed 6 May 2021].
- Jagpreet Sandhu (2019). *Black or blue solar panels: Which is better for your home?* [online] Solar Reviews. Available at: <https://www.solarreviews.com/blog/black-or-blue-solar-panels-which-is-better-for-your-home> [Accessed 29 Apr. 2021].
- Julien, C.M. and Mauger, A. (2017). *Critical review on lithium-ion batteries: are they safe? Sustainable?* *Ionics*, 23(8), pp.1933–1947.
- K-TRONIX S.A. (2018). *BATERÍAS Niquel Cadmio POWER MX - KTRONIX*. [online] Ktronix.com.mx. Available at: <http://www.ktronix.com.mx/bateriasnicd.html> [Accessed 6 May 2021].
- LaCalle, A. (2021). *¿Qué es una interfaz?: importancia de una buena interfaz*. [online] Albertolacalle.com. Available at: <https://albertolacalle.com/hci/interfaz.htm> [Accessed 7 May 2021].
- Lee, T.B. (2020). *Battery prices have fallen 88 per cent over the last decade*. [online] Ars Technica. Available at: <https://arstechnica.com/science/2020/12/battery-prices-have-fallen-88-percent-over-the-last-decade/> [Accessed 5 May 2021].
- Letcher, T.M. (2018). *Why Solar Energy? A Comprehensive Guide to Solar Energy Systems*, [online] pp.3–16. Available at: <https://www.sciencedirect.com/science/article/pii/B9780128114797000014?via%3Dihub> [Accessed 3 May 2021].
- Let's Talk Science. (2019). *How does a lithium-Ion battery work?* [online] Available at: <https://letstalkscience.ca/educational-resources/stem-in-context/how-does-a-lithium-ion-battery-work> [Accessed 6 May 2021].

- Lillevilla. (2021). *Luoman Loiste - Lillevilla*. [online] Available at: <https://fi.lillevilla.com/tuote/luoman-loiste/> [Accessed 11 May 2021]
- Ling, S.J., Sanny, J. and Moebis, W. (2016). *Semiconductor Devices*. [online] Opentextbc.ca. Available at: <https://opentextbc.ca/universityphysicsv3openstax/chapter/semiconductor-devices/> [Accessed 6 May 2021].
- Lumen. (2011). *Redox Reactions / Biology for Majors I*. [online] Available at: <https://courses.lumenlearning.com/wmopen-biology1/chapter/redox-reactions/> [Accessed 4 May 2021].
- Lumen Learning. (2021). *17.5 Batteries and Fuel Cells | General College Chemistry II*. [online] Available at: <https://courses.lumenlearning.com/suny-mcc-chemistryformajors-2/chapter/batteries-and-fuel-cells-2/> [Accessed 11 May 2021].
- Marino, D. (2020). *Basic electronics - Diodes*. [online] Hebergementwebs.com. Available at: <https://www.hebergementwebs.com/basic-electronics-tutorial/basic-electronics-diodes> [Accessed 6 May 2021].
- Marsh, J. (2017). *Why are solar panels blue?* [online] Solar News. Available at: <https://news.energysage.com/why-are-solar-panels-blue/> [Accessed 29 Apr. 2021].
- Meteoria.fi. (2021). *Start - Meteorian*. [online] Available at: <https://meteoria.fi/en> [Accessed 18 May 2021].
- Modicon Modbus Protocol Reference Guide. (1996). [online]. Available at: https://modbus.org/docs/PI_MBUS_300.pdf.
- Modbus Organisation. (2020). *The Modbus Organization*. [online] Available at: <https://www.modbus.org/> [Accessed 28 Apr. 2021].
- Mpoweruk.com. (2021). *Battery Performance Characteristics - How to specify and test a battery*. [online] Available at: <https://www.mpoweruk.com/performance.htm> [Accessed 12 May 2021].
- National Instruments. (2021). *The Modbus Protocol In-Depth*. [online] Available at: <https://www.ni.com/fi-fi/innovations/white-papers/14/the-modbus-protocol-in-depth.html> [Accessed 28 Apr. 2021].

Nordicgalvanizers. (2019). *Corrosion of zinc coatings – Nordic Galvanizers*. [online] Available at: <http://nordicgalvanizers.com/corrosion-of-zinc-coatings/> [Accessed 4 May 2021].

Novia.fi. (2021). *Line Chart*. [online] Available at: http://iot.novia.fi/data/meteorologia_weather.html [Accessed 18 May 2021].

Nrel.gov. (2021). *Solar Energy Basics*. [online] Available at: <https://www.nrel.gov/research/re-solar.html> [Accessed 3 May 2021].

OEM. (2021). *Taipuisat yksikidepaneelit*. [online] Available at: <https://www.oem.fi/tuotteet/akku/aurinkopaneelit-ja-tarvikkeet/aurinkopaneelit--645159/taipuisat-yksikidepaneelit--626501> [Accessed 29 Apr. 2021].

Off Grid Europe. (2017). *What is a Lead-Acid battery?* [online] Available at: <https://www.off-grid-europe.com/info/lead-acid-battery/> [Accessed 11 May 2021].

OpenStax (2016). *17.5 Batteries and Fuel Cells*. [online] Opentextbc.ca. Available at: <https://opentextbc.ca/chemistry/chapter/17-5-batteries-and-fuel-cells/> [Accessed 4 May 2021].

Osha.gov. (2021). *Cadmium - Overview | Occupational Safety and Health Administration*. [online] Available at: <https://www.osha.gov/cadmium> [Accessed 6 May 2021].

Palermo, E. (2015). *How Do Batteries Work?* [online] livescience.com. Available at: <https://www.livescience.com/50657-how-batteries-work.html> [Accessed 4 May 2021].

Papouch Store. (2014). *AD4ETH: Ethernet measurement module*. [online] Papouch store s.r.o. Available at: <https://en.papouch.com/ad4eth-ethernet-measurement-module-p4607/> [Accessed 11 May 2021].

Podder, S. and Khan, Md.Z.R. (2016). Comparison of lead acid and Li-ion battery in solar home system of Bangladesh. *2016 5th International Conference on Informatics, Electronics and Vision (ICIEV)*. [online] Available at: <https://ieeexplore.ieee.org/document/7760041/> [Accessed 10 May 2021].

PowerStream. (2021). *Alkaline Battery Chemistry Tutorial and FAQ from PowerStream describes the chemical properties of manganese dioxide zinc cells with alkaline hydroxide*

electrolytes. [online] Available at: <https://www.powerstream.com/BatteryFAQ-alkaline.html> [Accessed 4 May 2021].

PowerStream. (2021). *Lithium ion Battery Chemistry Tutorial and FAQ from PowerStream describes the chemical properties of lithium ion secondary cells*. [online] Available at: <https://www.powerstream.com/BatteryFAQ-lithium-ion.html> [Accessed 6 May 2021].

PowerStream. (2021). *Nickel-Cadmium Battery Chemistry Tutorial and FAQ from PowerStream describes the chemical properties of nickel-cadmium secondary cells*. [online] Available at: <https://www.powerstream.com/BatteryFAQ-nickel-cadmium.html> [Accessed 4 May 2021].

Process Industry Forum. (2019). *Why Choose Renewable Energy? | Renewable Energy Solutions*. [online] Available at: <https://www.processindustryforum.com/article/why-choose-renewable-energy> [Accessed 3 May 2021].

Proyecto investigación de Tecnología (2021). *Uniones P-N - Proyecto investigación de Tecnología*. [online] Google.com. Available at: <https://sites.google.com/site/tecnoiesvillena/elementos-activos/los-transistores/uniones-p-n> [Accessed 6 May 2021].

Rebacas (2020). *Batería de gel o Agm que las diferencia?* [online] Available at: https://www.rebacas.com/blog-baterias/39_bateria-de-gel-o-agm-que-las-diferencia-.html [Accessed 9 May 2021].

Robotica. (2021). *Laboratori de Robòtica, UdL*. [online] Available at: <http://robotica.udl.cat/simulador/> [Accessed 7 May 2021].

Sciencedirect. (2017). *Manganese Dioxide - an overview | ScienceDirect Topics*. [online] Available at: <https://www.sciencedirect.com/topics/engineering/manganese-dioxide> [Accessed 4 May 2021].

Sciencing. (2020). *Parts of a Battery*. [online] Available at: <https://sciencing.com/parts-battery-5419189.html> [Accessed 4 May 2021].

SEIA. (2019). *Solar Industry Research Data | SEIA*. [online] Available at: <https://www.seia.org/solar-industry-research-data> [Accessed 3 May 2021].

Sendy, A. (2017). *Types of solar panels: which one is the best choice?* [online] Solar Reviews. Available at: <https://www.solarreviews.com/blog/pros-and-cons-of-monocrystalline-vs-polycrystalline-solar-panels> [Accessed 29 Apr. 2021].

Sensata Technologies. (2021). *Inverter/Chargers and Charge Controllers: Do You Need Both? | Magnum Dimensions*. [online] Available at: <https://www.magnum-dimensions.com/knowledge/pvstorage/inverterchargers-and-charge-controllers-do-you-need-both> [Accessed 28 Apr. 2021].

Sergio Fernández Munguía (2017). *El mercado de la energía solar y el almacenamiento eléctrico superará los 49.000 millones en 2026*. [online] DiarioRenovables | Energías renovables. Eólica, solar, fotovoltaica, baterías, movilidad sostenible. Available at: <https://www.diariorenovables.com/2017/05/el-mercado-de-la-energia-solar-y-el-almacenamiento-electrico-superara-los-49.000-millones-en-2026.html> [Accessed 17 May 2021].

Shin, H. and Roh, J.H. (2020). Framework for Sizing of Energy Storage System Supplementing Photovoltaic Generation in Consideration of Battery Degradation. *IEEE Access*, [online] 8, pp.60246–60258. Available at: <https://ieeexplore.ieee.org/abstract/document/9023493> [Accessed 7 May 2021].

Silicon Lightworks (2016). *Silicon Lightworks*. [online] Available at: <https://siliconlightworks.com/li-ion-voltage> [Accessed 7 May 2021].

Tech Step Integration. (2020). *Modbus RTU Protocol Overview*. [online] Available at: <https://techstep.com.au/technologies/modbus-rtu/> [Accessed 28 Apr. 2021].

Treviño Quintillà, Marc and Zubieta Mor, Ion (2020). Automation Of A Solar Panel Test-Rig. *Theseus.fi*. [online] Available at: <https://www.theseus.fi/handle/10024/345272> [Accessed 19 May 2021].

Tuontitukku.fi. (2021). . [online] Available at: <https://www.tuontitukku.fi/rakentaminen-ja-varastointi/aurinkopaneeli-35w-taipuisa-70x35cm-kateva-joustava-paneeli-veneeseen/p/7350096340560/#description> [Accessed 29 Apr. 2021].

Victron Energy. (2020). *BMV-700 - Victron Energy*. [online] Available at: <https://www.victronenergy.com/battery-monitors/bmv-700> [Accessed 28 Apr. 2021].

Victron Energy. (2020). *Color Control GX - Victron Energy*. [online] Available at: <https://www.victronenergy.com/panel-systems-remote-monitoring/color-control> [Accessed 28 Apr. 2021].

Victron Energy. (2020). *SmartSolar MPPT 75/10, 75/15, 100/15 & 100/20 - Victron Energy*. [online] Available at: <https://www.victronenergy.com/solar-charge-controllers/smartsolar-mppt-75-10-75-15-100-15-100-20> [Accessed 28 Apr. 2021].




Volt Planet. (2021). *Victron Energy MultiPlus Inverter/Charger -12V 800W/35A*. [online] 12voltplanet.co.uk. Available at: <https://www.12voltplanet.co.uk/victron-energy-multiplus-invertercharger-12v-800w35a.html> [Accessed 28 Apr. 2021].



Wikiwand. (2021). Pila alcalina | Wikiwand. [online] Available at: https://www.wikiwand.com/es/Pila_alcalina [Accessed 7 May 2021].


Wikiwand. (2021). Pila de zinc-carbono | Wikiwand. [online] Available at: https://www.wikiwand.com/es/Pila_de_zinc-carbono [Accessed 7 May 2021].

8 Appendices

8.1 Appendix I – Overview table of the used components

Name	Manufacturer	Model	Description	Price	General link	Datasheet	Picture
Control Unit	Victron Energy	Color Control GX	Communication-centre of the installation. It offers at-a-glance live information and allows the control of all products connected to it.	510€	https://www.victronenergy.com/panel-systems-remote-monitoring/color-control	https://www.victronenergy.com/upload/documents/Datasheet-Color-Control-GX-EN.pdf	
Battery Monitor	Victron Energy	BMV-700	High precision battery monitor. The essential function of a battery monitor is to calculate ampere-hours consumed and the state of charge of a battery.	155€	https://www.victronenergy.com/battery-monitors/bmv-700	https://www.victronenergy.com/upload/documents/Datasheet-BMV-700-series-EN.pdf	
Inverter Charger	Victron Energy	Multi Compact 12/800/35-15	Powerful true sine wave inverter, a sophisticated battery charger that features adaptive charge technology and a high-speed AC transfer switch in a single compact unit.	555€	https://www.12voltplanet.co.uk/victron-energy-multiplus-invertercharger-12v-800w35a.html	https://www.off-grid-europe.com/downloads/dl/file/id/94/multiplus_datasheet.pdf	

Regulator	Victron Energy	Smart solar MPPT 75 10	Gathers energy from the solar panel, and stores it in your batteries. Using the latest, fastest technology, SmartSolar maximises this energy harvest, driving it intelligently to achieve full charge in the shortest possible time.	110€	https://www.victronenergy.com/solar-charge-controllers/smartsolar-mppt-75-10-75-15-100-15-100-20	https://www.victronenergy.com/upload/documents/Datasheet-SmartSolar-charge-controller-MPPT-75-10,-75-15,-100-15,-100-20_48V-EN.pdf	
PV panel	NORDMAX	NM35WFL	35 Watt NORDMAX thin-film PV panel with monocrystalline solar cells. Dimensions: 700 x 350 x 2.5 mm.	99€	https://www.tuontitukku.fi/pienkone-venen-ja-varaosa/aurinkopaneeli-35w-taipuisa-70x35cm-kateva-joustava-paneeli-veneseen/p/350096340560/	https://www.oem.fi/ui/product-resources/oem/-/-/154335.pdf?att=False&hash=A233653CCA78922BEE064A603023B877	

Battery	POWERXON	AGM 51Ah	Absorbed Glass Material battery, supply of 12VDC with a maximum output current of 12.5A	118€	https://nordso-lar.fi/tuote/powerxon-51ah-agm-akku/	https://www.fffgridtec.com/media/product_attachments/Datenblatt_2-01-001002_DE.pdf	
---------	----------	-------------	---	------	---	---	---

8.2 Appendix II – Block diagram of the LabVIEW program

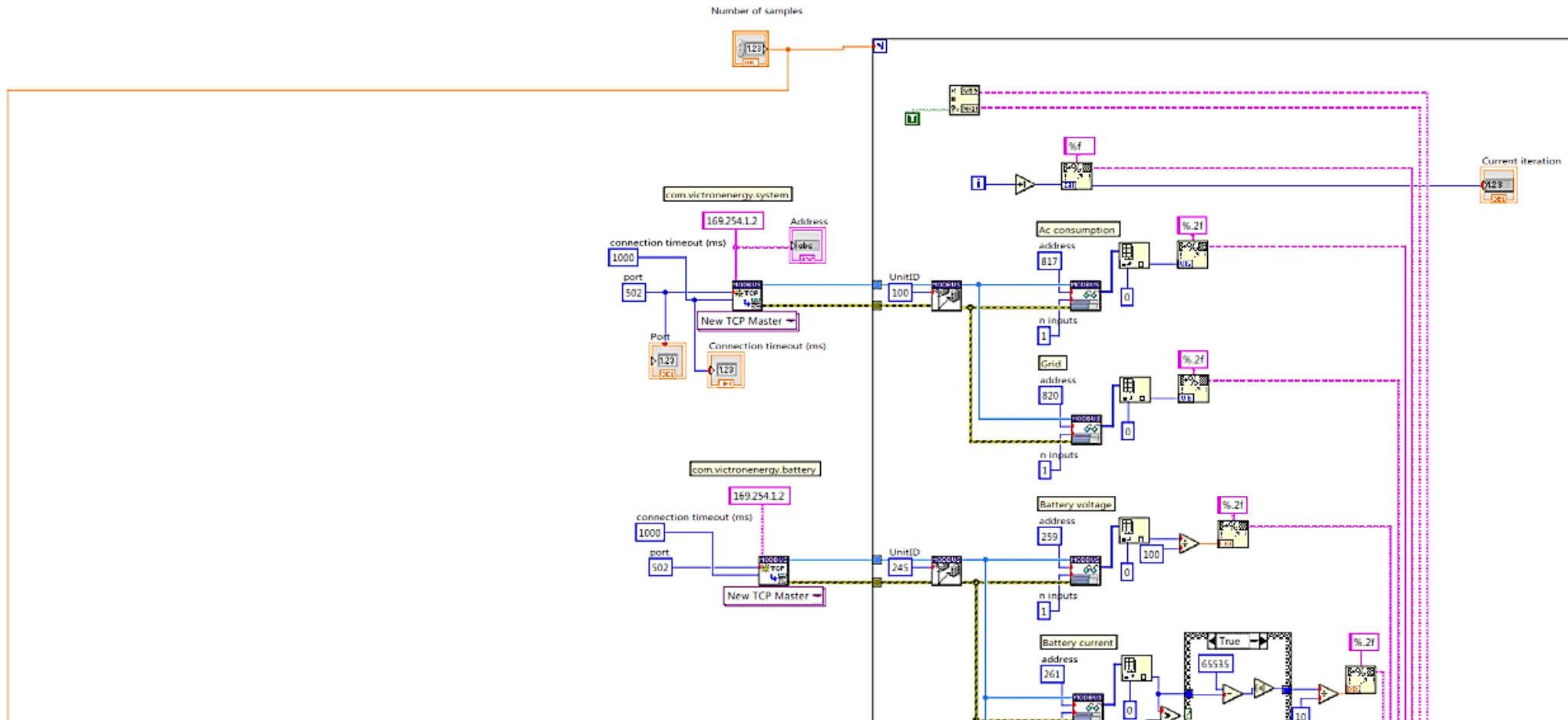


Figure 45. Final block diagram in LabVIEW (part 1)

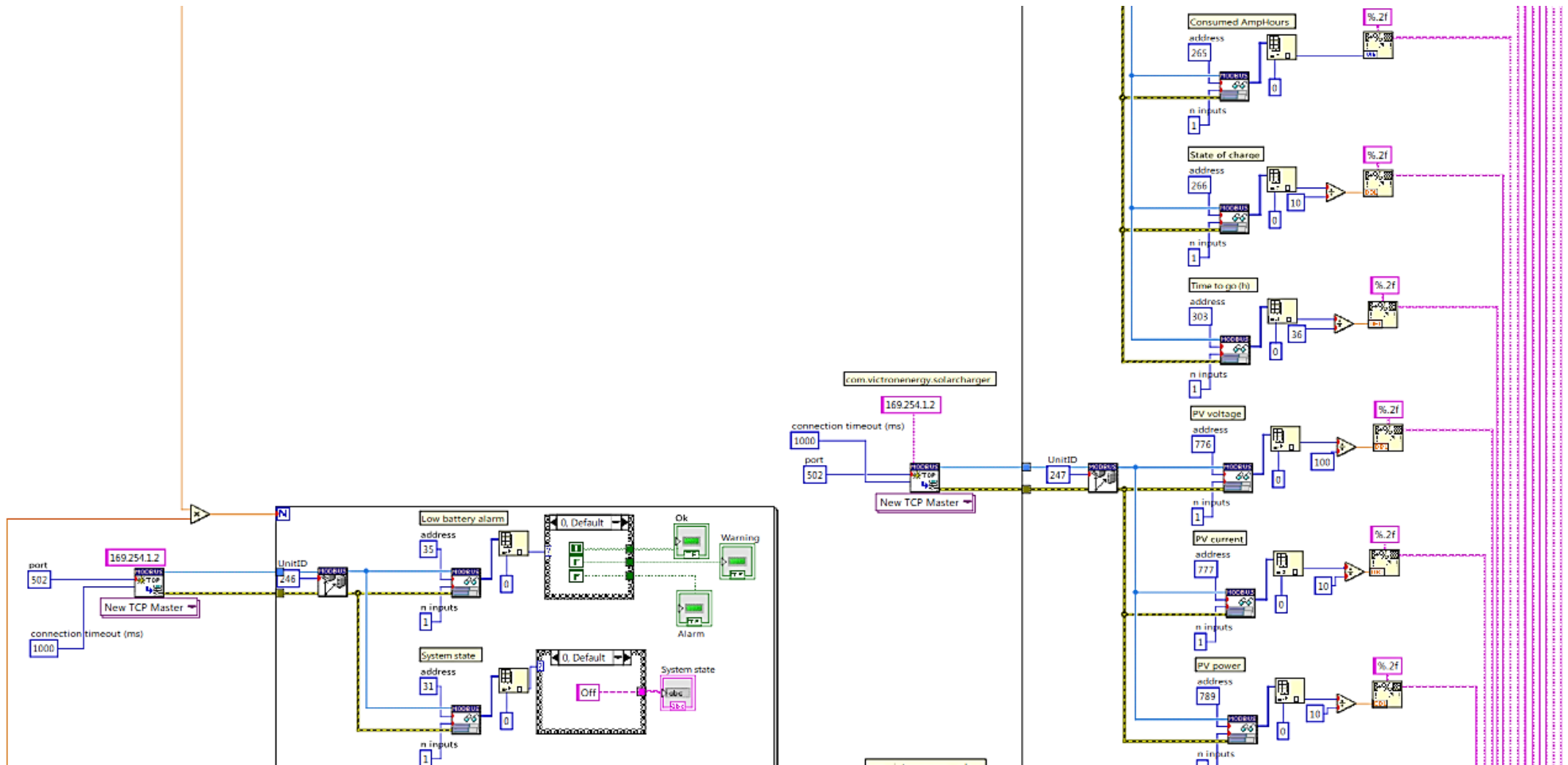


Figure 46. Final block diagram in LabVIEW (part 2)

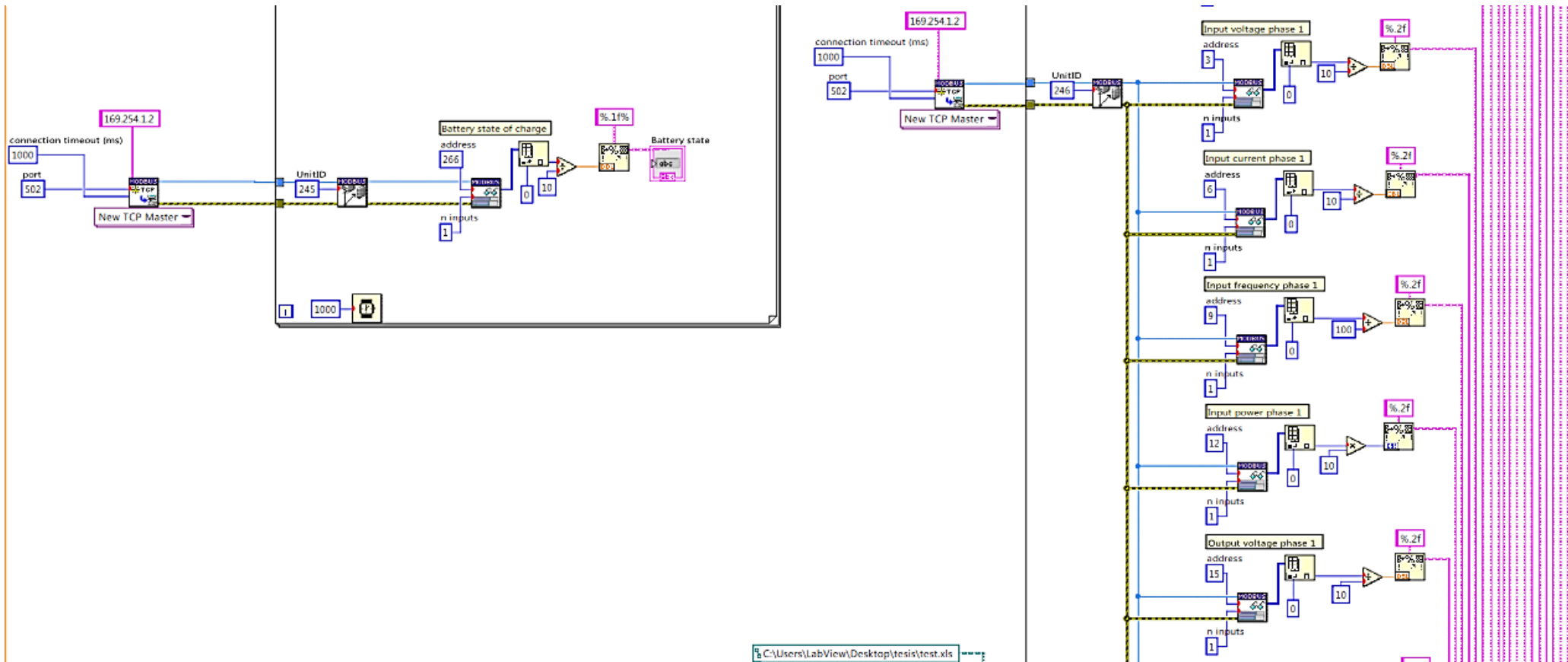


Figure 47. Final block diagram in LabVIEW (part 3)

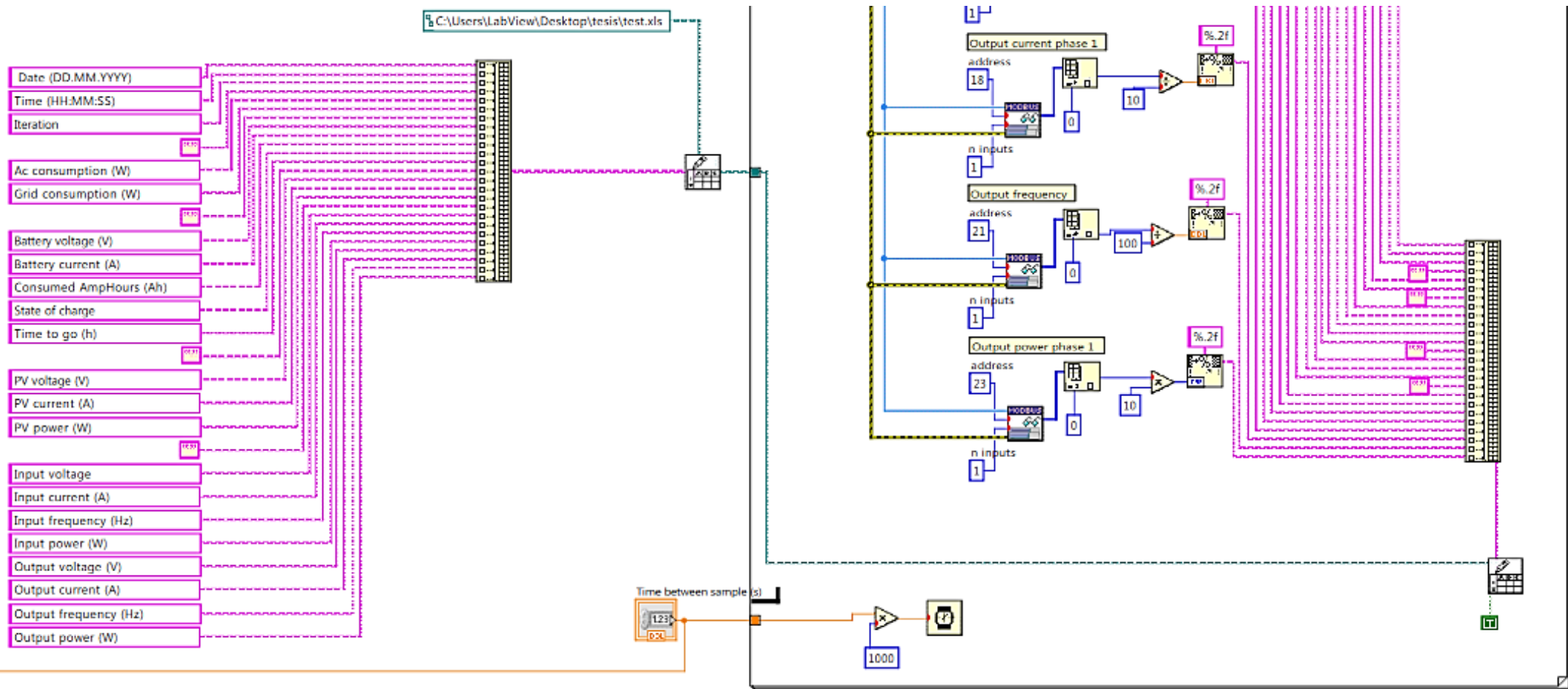


Figure 48. Final block diagram in LabVIEW (part 4)